Atmos. Chem. Phys., 23, 15165–15180, 2023
https://doi.org/10.5194/acp-23-15165-2023

Atmospheric Chemistry and Physics
Open Access
EGU

Research article

Comprehensive multiphase chlorine chemistry in the box model CAABA/MECCA: implications for atmospheric oxidative capacity

Meghna Soni[1,2], Rolf Sander[3], Lokesh K. Sahu[1], Domenico Taraborrelli[4], Pengfei Liu[5], Ankit Patel[6], Imran A. Girach[7], Andrea Pozzer[3,8], Sachin S. Gunthe[6,9], and Narendra Ojha[1]

[1]Space and Atmospheric Sciences Division, Physical Research Laboratory, Ahmedabad, India
[2]Indian Institute of Technology, Gandhinagar, India
[3]Atmospheric Chemistry Department, Max Planck Institute for Chemistry, Mainz, Germany
[4]Institute of Energy and Climate Research, Troposphere (IEK-8), Forschungszentrum Jülich GmbH, Jülich, Germany
[5]School of Earth and Atmospheric Sciences, Georgia Institute of Technology, Atlanta, GA, USA
[6]EE Division, Department of Civil Engineering, Indian Institute of Technology Madras, Chennai, India
[7]Space Applications Centre, Indian Space Research Organisation, Ahmedabad, India
[8]Climate and Atmosphere Research Center, The Cyprus Institute, Nicosia, Cyprus
[9]Centre for Atmospheric and Climate Sciences, Indian Institute of Technology Madras, Chennai, India

Correspondence: Meghna Soni (soni.meghna95@gmail.com) and Rolf Sander (rolf.sander@mpic.de)

Received: 4 April 2023 – Discussion started: 26 April 2023
Revised: 21 October 2023 – Accepted: 25 October 2023 – Published: 13 December 2023

Abstract. Tropospheric chlorine chemistry can strongly impact the atmospheric oxidation capacity and composition, especially in urban environments. To account for these reactions, the gas- and aqueous-phase Cl chemistry of the community atmospheric chemistry box model Chemistry As A Boxmodel Application/Module Efficiently Calculating the Chemistry of the Atmosphere (CAABA/MECCA) has been extended. In particular, an explicit mechanism for $ClNO_2$ formation following N_2O_5 uptake to aerosols has been developed. The updated model has been applied to two urban environments with different concentrations of NO_x ($NO + NO_2$): New Delhi (India) and Leicester (United Kingdom). The model shows a sharp build-up of Cl at sunrise through Cl_2 photolysis in both the urban environments. Besides Cl_2 photolysis, ClO+NO reaction and photolysis of $ClNO_2$ and ClONO are also prominent sources of Cl in Leicester. High-NO_x conditions in Delhi tend to suppress the nighttime build-up of N_2O_5 due to titration of O_3 and thus lead to lower $ClNO_2$, in contrast to Leicester. Major loss of $ClNO_2$ is through its uptake on chloride, producing Cl_2, which consequently leads to the formation of Cl through photolysis. The reactivities of Cl and OH are much higher in Delhi; however, the Cl/OH reactivity ratio is up to ≈ 9 times greater in Leicester. The contribution of Cl to the atmospheric oxidation capacity is significant and even exceeds (by ≈ 2.9 times) that of OH during the morning hours in Leicester. Sensitivity simulations suggest that the additional consumption of volatile organic compounds (VOCs) due to active gas- and aqueous-phase chlorine chemistry enhances OH, HO_2, and RO_2 near sunrise. The simulation results of the updated model have important implications for future studies on atmospheric chemistry and urban air quality.

Published by Copernicus Publications on behalf of the European Geosciences Union.

1 Introduction

Chlorine (Cl) radicals are one of the most important players in the tropospheric chemistry (Seinfeld and Pandis, 2016; Ravishankara, 2009). Cl impacts the oxidative capacity of the atmosphere and radical cycling and, therefore, can significantly alter the atmospheric composition (Seinfeld and Pandis, 2016; Faxon and Allen, 2013). In comparison with hydroxyl (OH) radicals, the so-called atmospheric detergent, the much faster reaction rates of Cl with volatile organic compounds (VOCs) enhance the peroxy radical (RO_2) formation and, thereby, the production of ozone (O_3) and secondary organic aerosols (SOAs) (Qiu et al., 2019a; Choi et al., 2020). In addition, Cl radicals can also enhance the oxidation of climate-driving gases (such as methane and dimethyl sulfide) (Saiz-Lopez and von Glasow, 2012). Cl radicals are produced in the atmosphere through photochemistry involving heterogeneous reactions of Cl-containing gases and aerosols (Qiu et al., 2019a; Faxon and Allen, 2013). The major sources of Cl-containing species are anthropogenic activities in continental regions and sea salt aerosols in marine and coastal environments (von Glasow and Crutzen, 2007; Osthoff et al., 2008; Liao et al., 2014; Liu et al., 2017; Thornton et al., 2010; Gunthe et al., 2021; Zhang et al., 2022). The photolysis of reactive Cl-containing species, such as chlorine gas (Cl_2), hypochlorous acid (HOCl), nitryl chloride ($ClNO_2$), and chlorine nitrite (ClONO), and the reaction of hydrochloric acid (HCl) with OH are known to produce Cl radicals in the lower troposphere (Atkinson et al., 2007; Riedel et al., 2014). With the rise in anthropogenic activities, emissions of Cl-containing species have increased significantly across the globe (Lobert et al., 1999; Zhang et al., 2022), and hence the importance of Cl in local as well as regional atmospheric chemistry has become prominent.

Despite the aforementioned importance, Cl chemistry and the associated mechanisms, especially heterogeneous reactions in the lower troposphere, are not yet fully understood, and the effects of Cl on atmospheric composition, air quality, and oxidation capacity remain uncertain. Field measurements have revealed high concentrations of Cl species over inland regions in addition to coastal and polar regions (von Glasow and Crutzen, 2007; Osthoff et al., 2008; Liao et al., 2014; Liu et al., 2017; Thornton et al., 2010); however, quantitative understanding of continental sources remains poorly understood. This is due to the lack of the relevant heterogeneous and gas-phase chemistry in atmospheric photochemical models despite the range of chemical mechanism complexity used in 3-D chemistry transport models (Xue et al., 2015; Pawar et al., 2023; Pozzer et al., 2022). In addition, the chemistry of Cl compounds has been less studied using the laboratory/chamber experiments. Qiu et al. (2019b) showed that due to inadequate representation of heterogeneous Cl chemistry, the Community Multiscale Air Quality (CMAQ) model underestimated nitrate concentrations during daytime but overestimated during nighttime in Beijing, China. In addition, the uncertainties associated with emission inventories of Cl species can lead to inaccurate estimation of air composition (Zhang et al., 2022; Sharma et al., 2019). For example, Pawar et al. (2023) noticed that even after the inclusion of HCl emissions from trash burning, the levels of nitrate, sulfate, nitrous acid (HONO), etc., still deviated from the observations in Delhi, India, highlighting the need to include emissions from other sectors, such as industries. A few recent studies assessed the impacts of the gas-phase Cl chemistry by including gas-phase $ClNO_2$ reactions; for example, Xue et al. (2015) reported about a 25 % enhancement in the daytime oxidation of carbon monoxide and VOCs at a coastal site in East Asia. In the same region, the model predicted a 5 %–16 % enhancement in peak ozone with $ClNO_2$ ($\approx$ 50–200 pmol mol^{-1}) at a mountain top in Hong Kong, China (Wang et al., 2016). The measurements of Cl_2 (up to $\approx$ 450 pmol mol^{-1}) and $ClNO_2$ (up to $\approx$ 3.5 nmol mol^{-1}) were reported from a rural site in the North China Plain, and Cl chemistry was shown to enhance the formation of peroxy radicals (by 15 %) and O_3 production rate (by 19 %) (Liu et al., 2017).

Nevertheless, the heterogeneous chemistry of Cl species remains poorly represented in models and often neglected in large-scale numerical simulations. For example, in several models, the heterogeneous uptake of N_2O_5 on aqueous aerosols yielded nitric acid (HNO_3) via reaction HET1:

$$N_2O_5(g) + H_2O(aq) \rightarrow 2HNO_3(aq). \quad (1)$$

However, N_2O_5 uptake on chloride-containing particles can produce $ClNO_2$ (Behnke et al., 1997; Thornton et al., 2010), especially in urban environments with strong NO_x emissions (Osthoff et al., 2008; Young et al., 2012). Incorporating heterogeneous mechanism of $ClNO_2$ into the regional models led to a 3 %–12 % increase in O_3 over northern China (Sarwar et al., 2014; Zhang et al., 2017; Liu et al., 2017). In addition, heterogeneous reactions of Cl-containing species including particulate chloride (pCl^-), Cl_2, $ClNO_2$, chlorine nitrate ($ClNO_3$), and hypochlorous acid (HOCl) are suggested to result in the formation of Cl radicals as well as in recycling of NO_x and HO_x (OH and HO_2) (Ravishankara, 2009; Qiu et al., 2019a; Hossaini et al., 2016; Faxon and Allen, 2013). Very recent measurements suggest a reduction in $ClNO_2$ formation due to the competition of N_2O_5 uptake among chloride, sulfate, and acetate aerosols (Staudt et al., 2019). These heterogeneous reactions can be of paramount significance in the Cl budget; however, to the best of our knowledge, these have not yet been considered in model simulations.

The main goal of the present study is to investigate the role of chlorine chemistry in chemically contrasting urban environments. In this regard, we incorporate comprehensive gas-phase and heterogeneous Cl chemistry into a state-of-the-art box model. Section 2 provides a detailed description of the Cl chemistry mechanism with gas-phase and heterogeneous reactions. Section 3 describes the model setup, and

Sect. 4 shows the simulation results which include a detailed investigation on (i) the sensitivity of air composition to chlorine chemistry, (ii) the production and loss of Cl and $ClNO_2$, (iii) the role of Cl in the atmospheric oxidative capacity (AOC), and (iv) the sensitivity to $ClNO_2 + Cl^-$ reaction.

2 Mechanism development

The community box model Chemistry As A Boxmodel Application/Module Efficiently Calculating the Chemistry of the Atmosphere (CAABA/MECCA, Sander et al., 2019), has been used in this work. A comprehensive gas- and aqueous-phase mechanism of chlorine chemistry has been added to MECCA, here used within the box model CAABA. The gas-phase and heterogeneous chemistry implemented in MECCA is described in the following subsections, and the full mechanism is shown in the Supplement.

2.1 Gas-phase chlorine chemistry

A total of 36 inorganic, organic, and photolysis reactions which are key contributors of Cl radicals were added to the mechanism (Table 1). The mechanism includes the inorganic reactions of Cl with NO_x, NO_3 (G1–G4), the reactions of Cl-containing species with OH and NO (G5–G7), and the reactions between Cl-containing species (G8–G9) (Qiu et al., 2019a; Burkholder et al., 2015; Atkinson et al., 2007). ClONO is formed through the reaction of Cl with NO_2 (G2) and exists as a metastable intermediate (Janowski et al., 1977; Niki et al., 1978; Golden, 2007). This intermediate subsequently transforms into $ClNO_2$ (G10), with an average conversion time of ≈ 12 h (ranging from 4 to 20 h), and the corresponding rate constant is $2.3 \times 10^{-5}\ s^{-1}$ (Janowski et al., 1977). The Cl-initiated oxidation of organic species, i.e., alkanes (C_3H_8, C_4H_{10}), aromatics (benzene (C_6H_6), toluene (C_7H_8) and xylene (C_8H_{10})), alcohols (CH_3OH, C_2H_5OH), ketones (CH_3COCH_3, MEK), isoprene (C_5H_8), and other organic compounds (C_2H_5CHO, $HOCH_2CHO$, BENZAL, GLYOX, MGLYOX), has also been included (G11–G31). The corresponding kinetic data are based on the International Union of Pure and Applied Chemistry and NASA Jet Propulsion Laboratory data evaluations (Atkinson et al., 2006, 2007; Burkholder et al., 2015), as well as from the literature (Niki et al., 1985, 1987; Green et al., 1990; Shi and Bernhard, 1997; Sokolov et al., 1999; Thiault et al., 2002; Wang et al., 2005; Rickard, 2009; Wennberg et al., 2018). In addition, photolysis reactions (G32–G36) resulting in production the of Cl are also added to the module (Atkinson et al., 2007). The abbreviations of species mentioned in Table 1 are kept similar to that in the Master Chemical Mechanism (MCM) nomenclature (Rickard, 2009).

2.2 Heterogeneous chemistry

The aqueous-phase and heterogeneous chemistry of Cl compounds added to MECCA is described in Table 2. In the present study, we assume that N_2O_5 is in equilibrium between the gas and aqueous phase (H2) according to Henry's law, and the dissociation of N_2O_5(aq) to nitronium ion (NO_2^+) and nitrate (NO_3^-) occurs according to Reaction (A1). The rate constant for the recombination reaction of NO_2^+ and NO_3^- is $2.7 \times 10^8\ mol^{-1}\ L\ s^{-1}$, calculated based on Bertram and Thornton (2009) and Staudt et al. (2019). The acid dissociation of nitric acid (HNO_3) in aqueous phase (A3) also results in the formation of NO_2^+ (Sapoli et al., 1985).

Thus, produced nitronium ion (NO_2^+) reacts reversibly with chloride (Cl^-), yielding $ClNO_2$ (A4, A5) (Staudt et al., 2019; Behnke et al., 1997). After outgassing according to Henry's law (H3), $ClNO_2$ is photolyzed in the gas phase, producing Cl and NO_2 (Ghosh et al., 2012; Sander et al., 2014). $ClNO_2$ uptake on chloride-containing aerosols results in the formation of Cl_2 and nitrite ion (NO_2^-), as shown by Reaction (A6) (Roberts et al., 2008). Chamber experiments suggest the formation of Cl_2 from the self-reaction of $OH{\cdot}Cl^-$ (A7), which gets formed via the reaction of OH with Cl^- (Knipping et al., 2000). Through another channel of reversible Reactions (A8, A9), $OH \cdot Cl^-$ reacts with aqueous chloride and produces Cl_2^-, which can yield Cl_2 through subsequent reactions (Grigorev et al., 1987). The NO_2^+ uptake on aqueous chloride to form $ClNO_2$ (A4) is ≈ 500 times faster than NO_2^+ reaction with H_2O (A10) (Staudt et al., 2019). At the same time, experimental studies revealed a strong competition of NO_2^+ to react with Cl^- and with other nucleophiles (e.g., SO_4^{2-}) and aqueous organic compounds, e.g., phenol, methanol, and cresol (A11–A16) (Staudt et al., 2019; Ryder et al., 2015; Heal et al., 2007; Iraci et al., 2007; Coombes et al., 1979). These reactions could suppress the formation of $ClNO_2$, and also the corresponding rate constants for Reactions (A11)–(A14) are similar to the $NO_2^+ + Cl^-$ reaction yielding $ClNO_2$, i.e., $7.5 \times 10^9\ mol^{-1}\ L\ s^{-1}$ (Staudt et al., 2019; Ryder et al., 2015; Heal et al., 2007). Methanol reacts with NO_2^+ (A15) and forms aqueous methyl nitrate (CH_3NO_3) (Iraci et al., 2007). Phase exchange for CH_3NO_3 and nitrophenol ($HOC_6H_4NO_2$) is shown by Reactions (H4) and (H5), respectively. The heterogeneous chemistry just discussed is implemented in MECCA and is summarized in Fig. 1. The rate constant for the NO_2^+ reaction with methoxyphenol is about $\approx 10\,000$ times smaller than the NO_2^+ + phenol reaction (Kroflič et al., 2015), so it is not considered in this study. In addition, nitration reactions of other alcohols (e.g., catechol and polyphenols) could be potentially important; however, due to unavailability of corresponding rate constants, these reactions are not considered in this study; nonetheless, future studies calculating the kinetics of these reactions are recommended.

Table 1. Gas-phase chlorine reactions and corresponding rate constants added to MECCA. The rate constants are expressed in units of cubic centimeters per molecule per second (cm^3 $molecule^{-1}$ s^{-1}) unless otherwise specified. Model-simulated maximum noontime J values for Delhi are provided.

Reaction		Rate constant	Reference
Inorganic reactions			
(G1)	$Cl + NO + M \rightarrow ClNO$	$7.6E(-32) \cdot (T/300)^{-1.8}$	Qiu et al. (2019a)
(G2)	$Cl + NO_2 + M \rightarrow ClONO$	1.6×10^{-11}	Burkholder et al. (2015)
(G3)	$Cl + NO_2 + M \rightarrow ClNO_2$	3.6×10^{-12}	Burkholder et al. (2015)
(G4)	$Cl + NO_3 \rightarrow ClO + NO_2$	2.40×10^{-11} Qiu et al. (2019a)	
(G5)	$Cl_2 + OH \rightarrow HOCl + Cl$	$3.6 \times 10^{-12} \cdot \exp(-1200/T)$	Atkinson et al. (2007)
(G6)	$ClNO_2 + OH \rightarrow HOCl + NO2$	$2.4 \times 10^{-12} \cdot \exp(-1250/T)$	Atkinson et al. (2007)
(G7)	$OClO + NO \rightarrow NO_2 + ClO$	$1.1 \times 10^{-13} \cdot \exp(350/T)$	Atkinson et al. (2007)
(G8)	$Cl + Cl_2O \rightarrow Cl_2 + ClO$	$6.2 \times 10^{-11} \cdot \exp(130/T)$	Atkinson et al. (2007)
(G9)	$ClO + OClO + M \rightarrow Cl_2O_3$	1.2×10^{-12}	Atkinson et al. (2007)
(G10)	$ClONO \rightarrow ClNO_2$	2.3×10^{-5} s^{-1}	Janowski et al. (1977)
Organic reactions			
(G11)	$Cl + C_3H_8 \rightarrow$ iso-$C_3H_7O_2 + HCl$	$1.4 \times 10^{-10} \cdot 0.43 \cdot \exp(75/T)$	Rickard (2009)
(G12)	$Cl + C_3H_8 \rightarrow$ n-$C_3H_7O_2 + HCl$	$1.4 \times 10^{-10} \cdot 0.59 \cdot \exp(-90/T)$	Rickard (2009)
(G13)	$Cl +$ iso-$C_4H_{10} \rightarrow$ iso-$C_4H_9O_2 + HCl$	$1.43 \times 10^{-10} \cdot 0.564$	Rickard (2009)
(G14)	$Cl +$ iso-$C_4H_{10} \rightarrow$ tert-$C_4H_9O_2 + HCl$	$1.43 \times 10^{-10} \cdot 0.436$	Rickard (2009)
(G15)	$Cl +$ n-$C_4H_{10} \rightarrow LC_4H_9O_2 + HCl$	2.05×10^{-10}	Atkinson et al. (2006), Rickard (2009)
(G16)	$Cl +$ benzene $\rightarrow C_6H_5O_2 + HCl$	1.3E-16	Sokolov et al. (1999)
(G17)	$Cl +$ toluene $\rightarrow C_6H_5CH_2O_2 + HCl$	6.20×10^{-11}	Wang et al. (2005)
(G18)	$Cl +$ isoprene $\rightarrow$ .63 LISOPAB + .30 LISOPCD + .07 LISOPEFO2 + HCl	$7.6 \times 10^{-11} \cdot \exp(500/T) \cdot 1.1 \cdot \exp(-595/T)$	Wennberg et al. (2018)
(G19)	$Cl +$ isoprene $\rightarrow$ .63 LISOPAB + .30 LISOPCD + .07 LISOPEFO2 + LCHLORINE	$7.6 \times 10^{-11} \cdot \exp(500/T) \cdot (1-1.1 \cdot \exp(-595/T))$	Wennberg et al. (2018)
(G20)	$Cl +$ xylene $\rightarrow C_6H_5CH_2O_2 +$ LCARBON $+ HCl$	1.50×10^{-10}	Shi and Bernhard (1997)
(G21)	$Cl + CH_3OH \rightarrow HOCH_2O_2 + HCl$	$7.1 \times 10^{-11} \cdot 0.59 \cdot \exp(-75/T)$	Atkinson et al. (2006)
(G22)	$Cl + C_2H_5OH \rightarrow HOCH_2CH_2O_2 + HCl$	$6.0 \times 10^{-11} \cdot \exp(155/T) \cdot 0.28 \cdot \exp(-350/T)$	Atkinson et al. (2006)
(G23)	$Cl + C_2H_5OH \rightarrow C_2H_5O_2 + HCl$	$6.0 \times 10^{-11} \cdot \exp(155/T) \cdot (1-0.28 \cdot \exp(-350/T))$	Atkinson et al. (2006)
(G24)	$Cl + HOCH_2CHO \rightarrow HOCHCHO + HCl$	$8.0 \times 10^{-12}/0.9 \cdot 0.35$	Atkinson et al. (2006), Niki et al. (1987)
(G25)	$Cl + HOCH_2CHO \rightarrow HOCH_2CO + HCl$	$8.0 \times 10^{-12}/0.9 \cdot (1-0.35)$	Atkinson et al. (2006), Niki et al. (1987)
(G26)	$Cl +$ GLYOX $\rightarrow$ HCOCO $+ HCl$	3.8×10^{-11}	Niki et al. (1985)
(G27)	$Cl +$ MGLYOX $\rightarrow CH_3CO + CO + HCl$	4.8×10^{-11}	Green et al. (1990)
(G28)	$Cl + C_2H_5CHO \rightarrow C_2H_5CO_3 + HCl$	1.3×10^{-10}	Atkinson et al. (2006)
(G29)	$Cl + CH_3COCH_3 \rightarrow CH_3COCH_2O_2 + HCl$	$1.5 \times 10^{-11} \cdot \exp(-590/T)$	Atkinson et al. (2006)
(G30)	$Cl +$ MEK $\rightarrow$ LMEKO$_2$ $+ HCl$	$3.05 \times 10^{-11} \cdot \exp(80/T)$	Atkinson et al. (2006)
(G31)	$Cl +$ BENZAL $\rightarrow C_6H_5CO_3 + HCl$	1.0×10^{-10}	Thiault et al. (2002)
Photolysis reactions		J value (s^{-1})	
(G32)	$ClO \rightarrow Cl +$ O3P	1.45×10^{-4}	Atkinson et al. (2007)
(G33)	$Cl_2O \rightarrow Cl + ClO$	9.20×10^{-4}	Atkinson et al. (2007)
(G34)	$Cl_2O_3 \rightarrow ClO + ClO_2$	5.50×10^{-4}	Atkinson et al. (2007)
(G35)	$ClNO \rightarrow Cl + NO$	2.89×10^{-3}	Atkinson et al. (2007)
(G36)	$ClONO \rightarrow Cl + NO_2$	3.81×10^{-3}	Atkinson et al. (2007)

In this study, Cl reacts with hydrocarbons and acetone via H abstraction and hence does not lead to the formation of any Cl-containing molecules, such as chloroacetone. This means that there are no such reactions in MECCA in which the Cl atom becomes part of the organic molecule. The reaction of Cl atoms with isoprene proceeds mainly via addition, and it produces chlorine-containing organics (Ragains and Finlayson-Pitts, 1997; Fan and Zhang, 2004). However, here we have simplified the mechanism by not considering the fate of organohalogens. Therefore, for future research,

Table 2. Aqueous-phase and heterogeneous chlorine reactions added to MECCA.

Reaction		Rate constant	Reference
Aqueous-phase reactions			
(A1)	$N_2O_5(aq) \rightarrow NO_2^+(aq) + NO_3^-(aq)$	$1.5 \times 10^5\ s^{-1}$	Staudt et al. (2019)
(A2)	$NO_2^+(aq) + NO_3^-(aq) \rightarrow N_2O_5(aq)$	$2.7 \times 10^8\ mol^{-1}\ L\ s^{-1}$	Bertram and Thornton (2009), Staudt et al. (2019)
(A3)	$HNO_3(aq) + H^+(aq) \rightarrow NO_2^+(aq) + H_2O(aq)$	$1.6 \times 10^9\ mol^{-1}\ L\ s^{-1}$	Sapoli et al. (1985)
(A4)	$NO_2^+(aq) + Cl^-(aq) \rightarrow ClNO_2(aq)$	$7.5 \times 10^9\ mol^{-1}\ L\ s^{-1}$	Staudt et al. (2019)
(A5)	$ClNO_2(aq) \rightarrow NO_2^+(aq) + Cl^-(aq)$	$2.70 \times 10^2\ s^{-1}$	Behnke et al. (1997)
(A6)	$ClNO_2(aq) + Cl^-(aq) \rightarrow Cl_2(aq) + NO_2^-(aq)$	$10^7\ mol^{-1}\ L\ s^{-1}$	Roberts et al. (2008)
(A7)	$OH{\cdot}Cl^-(aq) + OH{\cdot}Cl^-(aq) \rightarrow Cl_2(aq) + 2\ OH^-(aq)$	$1.8 \times 10^9\ mol^{-1}\ L\ s^{-1}$	Knipping et al. (2000)
(A8)	$OH{\cdot}Cl^-(aq) + Cl^-(aq) \rightarrow Cl_2^-(aq) + 2\ OH^-(aq)$	$10^4\ mol^{-1}\ L\ s^{-1}$	Grigorev et al. (1987)
(A9)	$Cl_2^-(aq) + 2\ OH^-(aq) \rightarrow OH{\cdot}Cl^-(aq) + Cl^-(aq)$	$4.5 \times 10^7\ mol^{-1}\ L\ s^{-1}$	Grigorev et al. (1987)
(A10)	$NO_2^+(aq) + H_2O(aq) \rightarrow HNO_3(aq) + H^+(aq)$	$1.6 \times 10^7\ mol^{-1}\ L\ s^{-1}$	Staudt et al. (2019)
(A11)	$NO_2^+(aq) + SO_4^{2-}(aq) \rightarrow SO_4^{2-}(aq) + NO_3^-(aq) + 2\ H^+(aq)$	$7.5 \times 10^9\ mol^{-1}\ L\ s^{-1}$	Staudt et al. (2019)
(A12)	$NO_2^+(aq) + HCOO^-(aq) \rightarrow HCOO^-(aq) + NO_3^-(aq) + 2\ H^+(aq)$	$7.5 \times 10^9\ mol^{-1}\ L\ s^{-1}$	Staudt et al. (2019)
(A13)	$NO_2^+(aq) + CH_3COO^-(aq) \rightarrow CH_3COO^-(aq) + NO_3^-(aq) + 2\ H^+(aq)$	$7.5 \times 10^9\ mol^{-1}\ L\ s^{-1}$	Staudt et al. (2019)
(A14)	$NO_2^+(aq) + phenol(aq) \rightarrow HOC_6H_4NO_2(aq) + H^+(aq)$	$7.5 \times 10^9\ mol^{-1}\ L\ s^{-1}$	Ryder et al. (2015), Heal et al. (2007)
(A15)	$NO_2^+(aq) + CH_3OH(aq) \rightarrow CH_3NO_3(aq) + H^+(aq)$	$4.5 \times 10^8\ mol^{-1}\ L\ s^{-1}$	Iraci et al. (2007)
(A16)	$NO_2^+(aq) + CRESOL(aq) \rightarrow TOL1OHNO2(aq) + H^+(aq)$	$7.5 \times 10^9\ mol^{-1}\ L\ s^{-1}$	Coombes et al. (1979)
Heterogeneous reactions		Henry's constant ($mol\ L^{-1}\ atm^{-1}$)	
(H2)	$N_2O_5(g) \rightleftharpoons N_2O_5(aq)$	8.8×10^2	Fried et al. (1994)
(H3)	$ClNO_2(g) \rightleftharpoons ClNO_2(aq)$	4.5×10^2	Frenzel et al. (1998)
(H4)	$HOC_6H_4NO_2(aq) \rightleftharpoons HOC_6H_4NO_2(g)$	8.9×10^1	Müller and Heal (2001)
(H5)	$CH_3NO_3(aq) \rightleftharpoons CH_3NO_3(g)$	2.0×10^0	Sander (2015)

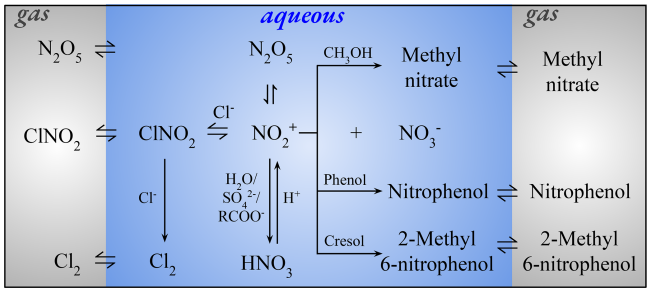

Figure 1. Aqueous-phase and heterogeneous chemistry added to MECCA.

it would be valuable to investigate the chemical kinetics of such reaction kinetics and their importance in the formation of organohalogen compounds.

3 Box model setup

The chemistry described in Sect. 2 has been added into community box model CAABA/MECCA v4.4.2 (Sander et al., 2019). A comprehensive gas- and aqueous-phase tropospheric chemistry involving a total of 3330 reactions was utilized for the simulations, and the full set of reactions are presented in the electronic supplement. The gas-phase chemistry of organics like terpenes and aromatics is treated by the Mainz Organic Mechanism (MOM) (Taraborrelli et al., 2012, 2021; Nölscher et al., 2014; Hens et al., 2014). The aqueous-phase chemistry of oxygenated VOCs is treated by the Jülich Atmospheric Mechanism of Organic Chemistry (JAMOC) (Rosanka et al., 2021). The numerical integration of the chemical mechanism is performed by the kinetic preprocessor v2.1 (KPP) (Sandu and Sander, 2006). The photolysis rate constants (J values) are calculated by the submodel JVAL, based on the method by Landgraf and Crutzen (1998). The Cl chemistry is expected to be more prominent during winter conditions due to the higher concentration of Cl-containing species in the boundary layer (Thornton et al., 2010; Gunthe et al., 2021; Sommariva et al., 2021), and, therefore, simulations are performed for the winter season. Hence, the model is set up for typical winter conditions of two different urban environments: Delhi (28.6° N, 77.2° E), India, and Leicester (52.4° N, 01.1° W), United Kingdom. Simulations are performed for a 5 d period (17–21 February 2018), and the output of the fifth day is considered for the analysis; by then, radicals have achieved an almost steady state. The typical environmental conditions used in the simulations for Delhi (Tripathi et al., 2022) and Leicester (Sommariva et al., 2021) are summarized in Tables 3 and S1.

VOC emissions are taken from the CAMS inventory (Sindelarova et al., 2014; Granier et al., 2019) and are adjusted iteratively in magnitude for better agreement with observations. CAMS-GLOB-ANT v5.3 (0.1° × 0.1°) (Granier et al., 2019) provides emissions of anthropogenic VOCs (e.g., benzene and toluene), while emissions of biogenic VOCs (e.g.,

Table 3. Environmental conditions of Delhi and Leicester in the model simulations.

Parameter	Delhi	Leicester
Latitude	28.58° N	52.38° N
Longitude	77.22° E	01.08° W
Time zone	GMT+5:30	GMT+0:00
Temperature (K)	292	278.1
Pressure (mbar)	1010	1004
Air number density (molecules cm^{-3})	2.5×10^{19}	2.61×10^{19}
Relative humidity	67 %	90 %

isoprene) are from CAMS-GLOB-BIO v3.1 (0.25° × 0.25°) (Sindelarova et al., 2014). Emissions of HCl and particulate chloride are included from Zhang et al. (2022) and adjusted iteratively towards reported levels of Cl-containing species (Gunthe et al., 2021; Sommariva et al., 2021). The Mainz Organic Mechanism (MOM) dry deposition scenario (Sander et al., 2019) is activated in the model. Ground-based lidar measurements of boundary layer height (BLH) during wintertime, performed as a part of the European Integrated project on Aerosol Cloud Climate and Air Quality Interactions (EUCAARI) project, are utilized for the simulations at Delhi (Nakoudi et al., 2019). The diurnal variation in BLH in Leicester is extracted from the European Centre for Medium-Range Weather Forecasts (ECMWF) fifth-generation reanalysis dataset ERA5 (Hersbach et al., 2020). Air composition in the model has been initialized based on previous studies (Table S1; Zhang et al., 2007; Lanz et al., 2010; Lawler et al., 2011; Sommariva et al., 2018, 2021; Gunthe et al., 2021; Tripathi et al., 2022). The values of aerosol properties (e.g., radius, liquid water content, and chemical composition) incorporated in the simulations for both Delhi and Leicester are provided in Table S1. We constrained the model with the parameterized function best representing the observed diurnal variations of NO_x (Fig. 2) (Tripathi et al. (2022); Sommariva et al. (2018, 2021), https://uk-air.defra.gov.uk/data/, last access: 4 December 2023), which helped in better reproducing the diurnal variations of some VOCs (e.g., isoprene) and ozone. Diurnal observations of HONO from Sommariva et al. (2021) are used for Leicester. For Delhi, however, HONO could not be constrained due to a lack of observations.

4 Results and discussion

The model captures the patterns in O_3 variability at both locations (Sommariva et al., 2018; Nelson et al., 2021; Chen et al., 2021; Sommariva et al., 2021; Nelson et al., 2023) to an extent, as shown in Fig. 2. O_3 is underestimated after ≈ 16:00 LT in Leicester, mainly due to titration by high NO and lack of adequate dynamics/transport of O_3 in the model. Entrainment seems to improve O_3 after midnight to-

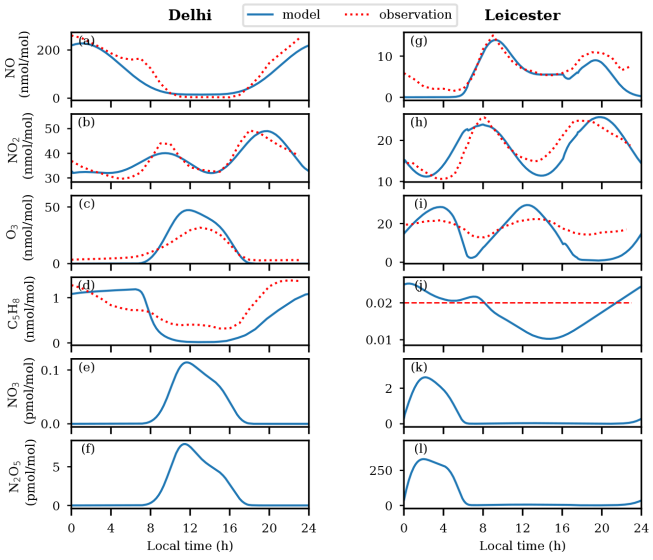

Figure 2. Diurnal variations of $NO, NO_2, O_3, C_5H_8, NO_3$, and N_2O_5 mixing ratios in Delhi **(a–f)** and Leicester **(g–l)**. The unusual and negligible nighttime NO_3 in Delhi is attributed to the nearly non-existent O_3, due to titration by higher concentrations of NO. This leads to the negligible nighttime N_2O_5 in this region. Although mixing ratios of NO_3 and N_2O_5 peak during the daytime, their levels remain quite low. The mean value of observed C_5H_8 in Leicester is shown by the red-colored long dashed line.

wards the observed values (Fig. 2i). Simulated isoprene is in agreement with diurnal observations in Delhi (Tripathi et al., 2022) and in accordance with the observed mean level in Leicester (Sommariva et al., 2021). The nitrate radical (NO_3), which is a nighttime oxidant, is formed through reaction between NO_2 and O_3 (G37). NO_3 can react with NO_2, forming N_2O_5, which can again produce NO_3 and NO_2 through thermal dissociation (G38).

$$NO_2 + O_3 \longrightarrow NO_3 + O_2 \quad \text{(G37)}$$

$$NO_3 + NO_2 + M \rightleftharpoons N_2O_5 + M \quad \text{(G38)}$$

As seen in Fig. 2e, NO_3 remains negligible during the nighttime (≈ 18:00–07:30 LT) in Delhi due to unavailability of O_3 under high-NO conditions (up to 200 nmol mol^{-1}). Interestingly, despite its very short lifetime (≈ 5 s), about ≈ 0.1 pmol mol^{-1} of NO_3 is sustained during daytime. This is primarily due to prevailing levels of NO_2 (≈ 30 nmol mol^{-1}) and O_3 (≈ 40 nmol mol^{-1}). Such unusual daytime enhanced NO_3 has been reported in recent studies, for example, 5–31 pmol mol^{-1} of NO_3 in Texas, USA (Geyer et al., 2003). Aircraft measurements during the New England Air Quality Study showed ≈ 0.5 pmol mol^{-1} of NO_3 within the boundary layer (≤ 1 km) during noontime (Brown et al.,

2005). The calculated NO_3 levels using steady-state approximation showed 0.01–0.06 pmol mol^{-1} of NO_3 for the 1997–2012 period at urban sites in the UK (Marylebone Road London, London Eltham, and Harwell) (Khan et al., 2015a). Horowitz et al. (2007) suggested that NO_3 in tenths of picomoles per mole (pmol mol^{-1}) during daytime over the eastern United States results in the formation of $\approx 50\,\%$ isoprene nitrates through oxidation of isoprene, which could further affect the formation of O_3 and SOA significantly (Horowitz et al., 2007). Following to higher NO_3, up to 8 pmol mol^{-1} of N_2O_5 is simulated during daytime in Delhi (Fig. 2f). Similar unusual daytime high levels of N_2O_5 ($\approx 21.9 \pm 29.3$ pptv) during wintertime were recently measured at Delhi using a high-resolution iodide adduct chemical ionization mass spectrometer (Haslett et al., 2023).

Enhanced $NO_3 \approx 2.6$ pmol mol^{-1} and $N_2O_5 \approx 330$ pmol mol^{-1} are simulated after midnight in Leicester (Fig. 2k, l). In contrast to Delhi, the daytime simulated levels of NO_3 are negligible as it gets removed rapidly during the daytime by photolysis and through its reactions with NO, HO_2, RO_2, and VOCs (Khan et al., 2015b). In conjunction with high NO from $\approx$ 16:00 LT to near midnight that titrates O_3, the corresponding NO_3 and N_2O_5 is negligible (following Reactions G37 and G38). Nighttime high and negligible daytime levels of NO_3 and N_2O_5 are their typical features which are generally reported in the literature (Brown et al., 2001; Seinfeld and Pandis, 2016).

4.1 Sensitivity of air composition to chlorine chemistry

To investigate the effects of Cl chemistry on air composition, other than comprehensive chemistry simulation discussed in the previous section (simulation: NEW, i.e., chemistry already present in the model + newly added gas- and aqueous-phase chlorine chemistry), two additional simulations have been performed, which are (1) OLD (this includes the default chemistry already present in the model) and (2) NOCL (OLD minus chlorine chemistry, i.e., without Cl chemistry). The OLD simulation also encompassed some basic chlorine chemistry that was part of the model prior to its update (full mechanism is also shown in the Supplement). Figure 3 shows the comparison of Cl, $ClNO_2$, ClONO, OH, HO_2, and RO_2 variations among the three simulations in Delhi and Leicester. Figure S5 shows the differences in diurnal variations of Cl, ClONO + $ClNO_2$, OH, HO_2, and RO_2 in the NEW simulation with the NOCL and OLD simulations.

The Delhi environment is mainly characterized by two peaks in Cl, a predominant sharp peak just after sunrise followed by a broad shallow peak during noontime, corresponding to different mechanisms as discussed in the next section. With newly added chemistry (NEW simulation), a sharp peak in Cl is seen near sunrise, with the maximum values attained being ≈ 3.5 fmol mol^{-1} (8.75×10^4 molec cm^{-3}) in Delhi (Fig. 3a). A broad smaller peak with a magnitude of ≈ 0.8 fmol mol^{-1} maximizing around noontime is seen, which is ≈ 4 times smaller than the first morning peak. The OLD simulation also shows a sharp peak in Cl near sunrise in Delhi, with a maximum of ≈ 11 fmol mol^{-1} (2.75×10^5 molec cm^{-3}). Cl get suppressed by up to $\approx$ 0.01 pmol mol^{-1} of maximum value in the OLD simulation, in the presence of added chlorine chemistry (NEW) as shown in Fig. S5. Similar to Cl, a peak is seen in ClONO+$ClNO_2$ of ≈ 100 pmol mol^{-1} with sunrise, which gradually decreases and attains ≈ 7 pmol mol^{-1} from nearly 11:00–16:00 LT. Afterwards it increases to ≈ 20 pmol mol^{-1} from late evening as shown by Fig. 3b and c. The pathways for the formation of $ClNO_2$ and ClONO were absent in the earlier version of the model (OLD). Simulated OH, HO_2, and RO_2 show a prominent peak just after sunrise in the presence of Cl chemistry for both the OLD and NEW simulations (Fig. 3d, e, f). As a consequence of greater oxidation of VOCs by Cl, enhanced levels of OH by 0.05 pmol mol^{-1} (up to a factor of ≈ 1.8), HO_2 by 0.21 pmol mol^{-1}, and RO_2 by 0.1 pmol mol^{-1} are noted with added Cl chemistry compared to the NOCL case (see Fig. S5). No significant changes are seen in noontime levels of OH and HO_2, whereas ≈ 1.1 times more RO_2 is produced with added Cl chemistry (NEW) compared to the OLD simulation.

The model-predicted Cl peaks at ≈ 2 fmol mol^{-1} (5.2×10^4 molec cm^{-3}) during sunrise in Leicester (Fig. 3g). In contrast to Delhi, suppressed Cl (up to ≈ 3.2 times) with a

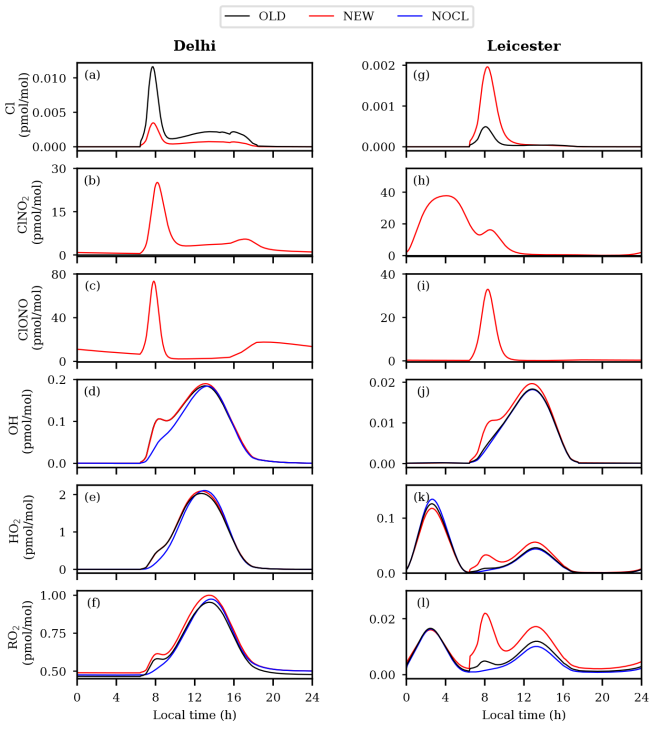

Figure 3. Model-simulated diurnal variations of Cl, $ClNO_2$, ClONO, OH, HO_2, and RO_2 at Delhi **(a–f)** and Leicester **(g–l)**.

narrow peak is simulated by the OLD simulation in comparison with the NEW simulation containing newly added Cl chemistry at Leicester. In contrast to negligible nighttime $ClONO + ClNO_2$ in Delhi, it shows a strong build-up over Leicester during 00:00–04:00 LT with a maximum of ≈ 40 pmol mol^{-1}, with higher levels (up to 50 pmol mol^{-1}) prevailing until about sunrise. $ClONO + ClNO_2$ is negligible during midday until midnight, in accordance with N_2O_5 in Leicester as shown in Fig. 2l. Previous studies have demonstrated that the formation of $ClNO_2$ occurs within the nocturnal residual layer, which contains lower levels of NO compared to the surface layer. Subsequently, $ClNO_2$ mixes downward during the morning when the convective mixed layer develops (Bannan et al., 2015; Tham et al., 2016). However, the present study does not account for the the effect of transport processes due to the limitations of the box model. The effects of added Cl chemistry on OH, HO_2, and RO_2 are more prominent in Leicester compared to Delhi. The NEW simulation shows strong enhancements in OH (up to ≈ 2 times), HO_2 (up to ≈ 5 times), and RO_2 (up to ≈ 8 times) after sunrise, which is gradually progressive, resulting in higher levels during noontime as well (Figs. 3, S5). Remarkably elevated levels of RO_2 (by a factor of ≈ 2) are prominent during the noon hours. Such elevated levels of RO_2 could favor enhanced levels of secondary organic aerosols in Leicester. The impact of Cl chemistry on aerosols (NO_2^+, NO_3^-, and oxalic acid) is discussed in Supplement Sect. 2.2 (Fig. S6). Though significant differences in NO_2^+, NO_3^-, and oxalic acid are seen due to Cl chemistry, further measurements are required for validation. In the next sections, we have analyzed the observed behavior of Cl and $ClNO_2$ in the NEW simulation over both the locations in more detail.

4.2 Production and loss of Cl and $ClNO_2$

The sources and sinks of Cl in Leicester and Delhi are presented in Fig. 4. Panel (a) delineates the sources and sinks of Cl radical on the diurnal scale in Delhi. The morning sharp peak in Cl radical is caused mainly by the photolysis of Cl_2 with a maximum rate of 1.2×10^7 molec cm^{-3} s^{-1}. The shallow secondary peak is due to the reaction $HCl + OH$ with a noontime rate of $\approx 0.4 \times 10^7$ molec cm^{-3} s^{-1}. However, there is a smaller contribution from other reactions (photolysis of $ClNO_2$, ClONO, and reaction of ClO with NO) to the morning peak, which have negligible contributions during the daytime. Interestingly, there is a strong consumption of Cl to oxidize VOCs (peak rate $\approx 2.4 \times 10^7$ molec cm^{-3} s^{-1}) during sunrise and a lesser consumption during the rest of the day. $Cl + NO_2$ is also a Cl sink during the morning time in Delhi. The Cl-initiated oxidation of VOCs in the morning hours in Delhi may lead to formation of secondary organic aerosols and new particle formation, which opens up pathways of future research in this direction. In addition to Cl_2 photolysis ($\approx 1.0 \times 10^6$ molec cm^{-3} s^{-1}), photolysis of $ClNO_2$ and ClONO as well as $ClO + NO$ reaction

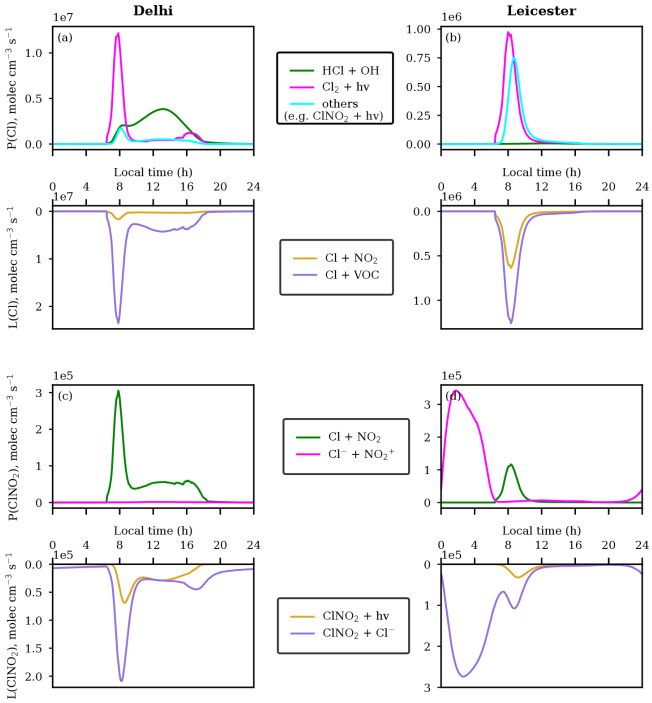

Figure 4. Production and loss rates of **(a, b)** Cl and **(c, d)** $ClNO_2$ in Delhi **(a, c)** and Leicester **(b, d)**.

(total rate $\approx 0.8 \times 10^6$ molec cm^{-3} s^{-1}) are other prominent sources of Cl in Leicester. VOCs are the major sink for Cl (rate $\approx 1.3 \times 10^6$ molec cm^{-3} s^{-1}), followed by NO_2 (rate $\approx 0.6 \times 10^6$ molec cm^{-3} s^{-1}).

We further analyzed the production and loss pathways of $ClNO_2$, as shown in Fig. 4c and d. While the major source of $ClNO_2$ is through the $Cl + NO_2$ reaction with a reaction rate $\approx 3 \times 10^5$ molec cm^{-3} s^{-1} in Delhi, the aqueous-phase reaction $Cl^- + NO_2^+$ ($\approx 3.4 \times 10^5$ molec cm^{-3} s^{-1}) is the prominent source in Leicester corresponding to the peak $ClNO_2$ (Fig. 2h, p). Though the gas-phase reaction $Cl + NO_2$ is discussed in the literature (Burkholder et al., 2015; Qiu et al., 2019a), to the best of our knowledge, such an unusually higher contribution of this reaction (seen in Delhi) as compared to the aqueous-phase reaction of $Cl^- + NO_2^+$ has not been reported in any study. The reaction of Cl with NO_2 ($\approx 1.1 \times 10^5$ molec cm^{-3} s^{-1}) is the major $ClNO_2$ source during sunrise in Leicester. In contrast, there is a lower contribution of the $Cl^- + NO_2^+$ reaction (rate $\approx 1 \times 10^3$ molec cm^{-3} s^{-1}) in $ClNO_2$ production in Delhi. The prominent sink for $ClNO_2$ is through its heterogeneous reaction with Cl^- ($\approx 1.8 \times 10^5$ molec cm^{-3} s^{-1} or 7.2×10^{-15} mol mol^{-1} s^{-1}) in Delhi almost throughout the day, while its loss through the photolysis ($\approx 0.5 \times 10^5$ molec cm^{-3} s^{-1} or 2×10^{-15} mol mol^{-1} s^{-1}) is also an important sink during the daytime. We are using $ClNO_2$ uptake coefficient $\gamma = 9 \times 10^{-3}$ from Fickert et al. (1998) in the simulation.

The sensitivity simulation with $\gamma = 1 \times 10^{-5}$ (Haskins et al., 2019) results in a considerably slower (by a factor of ≈ 270 and ≈ 17, near sunrise and during midday, respectively) loss rate of $ClNO_2$ with Cl^- than in the NEW simulation over Delhi. $ClNO_2$ loss through the reaction $ClNO_2 + Cl^-$ ($\approx 2.7 \times 10^5$ molec cm^{-3} s^{-1} or 1.0×10^{-14} mol mol^{-1} s^{-1}) is its major sink in Leicester from midnight to midday, while photolysis ($\approx 0.3 \times 10^5$ molec cm^{-3} s^{-1} or 1.1×10^{-15} mol mol^{-1} s^{-1}) is the smaller sink from sunrise to midday here. The diurnal variation in Cl_2 and its production and loss mechanisms over Delhi and Leicester are shown by Figs. S1 and S2. In conjunction with the major loss of $ClNO_2$, the $ClNO_2 + Cl^-$ reaction is the major contributor to Cl_2 formation over Delhi and Leicester.

We also calculated $ClNO_2$ yield from NO_2^+ (Fig. S3), which is the ratio of P_{ClNO_2}/L_{total}, where P_{ClNO_2} is the rate of $ClNO_2$ production through the Cl^- + NO_2^+ reaction and L_{total} denotes the loss rate of NO_2^+ through its reactions with Cl^-, H_2O, SO_4^{2-}, $HCOO^-$, CH_3COO^-, phenol, CH_3OH, and cresol (A4, A10–A16). $ClNO_2$ yield is ≈ 0.9 over Delhi, indicating the strongest loss of NO_2^+ is through its reaction with Cl^-, which is also mimicked in Fig. S4a, showing the same concentrations of $ClNO_2$ as in the NEW simulation and when other NO_2^+ reactions (A10–A16) are turned off (simulation: without other NO_2^+ reactions). $ClNO_2$ yield over Leicester is between ≈ 0.40 and 0.55, which is about half the yield in Delhi. Stronger $ClNO_2$ yield in Delhi could be attributed to ≈ 2 times higher Cl^- than Leicester. Lesser $ClNO_2$ yield in Leicester portrays the importance of NO_2^+ loss reactions (A10–A15) other than with Cl^-, which could be seen through Fig. S4b where $ClNO_2$ is increased by more than 2 times during the early morning hours when A10–A15 reactions are kept inactive in the model. The determination of $ClNO_2$ yield using cavity ring-down spectroscopy and chemical ionization mass spectrometry shows yield ranging between 0.2 and 0.8 for Cl^- concentrations of 0.02 to 0.5 mol L^{-1} (Roberts et al., 2009). The measurements of $ClNO_2$ yield for coastal and open-ocean waters were found to be between 0.16 and 0.30, which is suppressed by up to 5 times compared to equivalent salt containing solutions due to the addition of aromatic organic compounds (e.g., phenol and humic acid) to synthetic seawater matrices (Ryder et al., 2015).

4.3 Role of Cl in atmospheric oxidative capacity (AOC)

In order to understand the role of Cl as an oxidizing agent with respect to the OH radical, we calculated the reactivity of Cl and OH as Σ_{X_i} ($k_{\text{radical}+X_i} \times [X_i]$), where the radical is Cl or OH, and $[X_i]$ is the concentration of species X_i (here X_i includes CO, CH_4, primary VOCs, and NMHCs which are initialized in the model) (Fig. 5). The corresponding rate constants for $Cl + X_i$ and $OH + X_i$ reactions are taken from MECCA. The reactivity of both Cl and OH decreases rapidly nearly from sunrise to noontime and afterwards increases

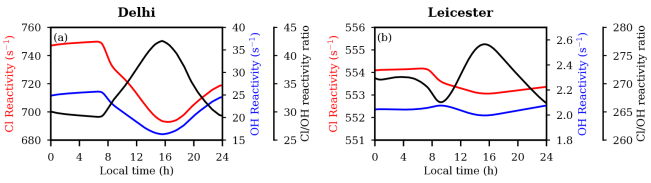

Figure 5. Reactivity of Cl and OH with CO, CH_4, and VOCs, as well as the Cl/OH reactivity ratio during the simulation period in **(a)** Delhi and **(b)** Leicester.

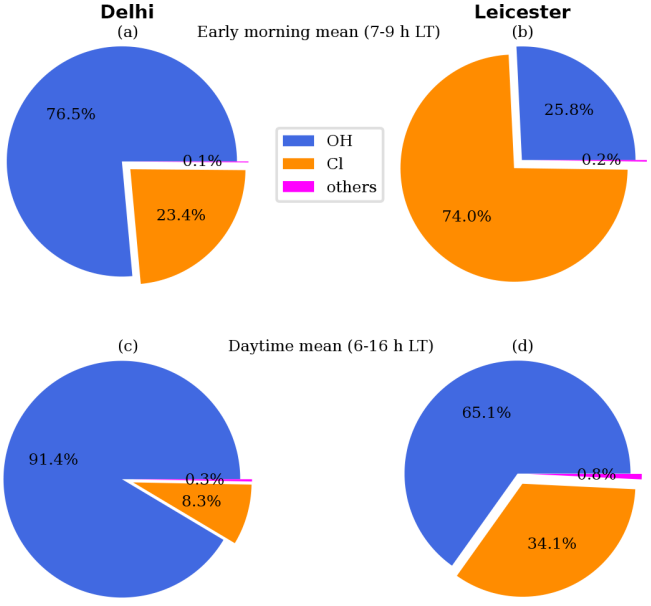

Figure 6. Atmospheric oxidative capacity (AOC) of radicals during **(a, b)** early morning mean (07:00–09:00 LT) and **(c, d)** daytime mean (06:00–16:00 LT) in Delhi **(a, c)** and Leicester **(b, d)**.

gradually at both locations. In comparison to Leicester, the magnitudes of Cl and OH reactivity in Delhi are higher by up to ≈ 1.4 and ≈ 12 times, respectively. However, the Cl/OH reactivity ratio in Leicester is up to ≈ 9 times higher than that in Delhi. Cl reactivity is lower (Delhi: ≈ 685 s^{-1}; Leicester: ≈ 553 s^{-1}) during noontime and higher (Delhi: ≈ 750 s^{-1}; Leicester: ≈ 554 s^{-1}) during nighttime and the early morning hours at both locations. The OH reactivity follows a similar pattern to that of Cl in Delhi and Leicester. The ratio of Cl to OH reactivity starts increasing after sunrise, reaching a maximum value of ≈ 42 at nearly 16:00 LT, and then decreases further in Delhi. As mentioned above, the Cl/OH reactivity ratio in Leicester shows a double peak pattern, with one peak (≈ 270) during the early morning $\approx 04:00$ LT and the other peak (≈ 276) at about 16:00 LT.

We quantified the relative contribution of Cl in atmospheric oxidative capacity (AOC) using the model. AOC represents the sum of oxidation rates of species X_i by oxidants Y (OH, Cl, and other radicals, NO_3 and O_3) (Elshorbany et al.,

2009):

$$\mathrm{AOC} = \sum k_{X_i}[X_i][Y] \quad (1)$$

where k_{X_i} is the corresponding rate constant for the $X_i + Y$ reaction. Accordingly, the magnitude of AOC depends upon the concentration and reactivity of Cl. Figure 6 shows the contribution of individual oxidants in AOC at both locations. Besides OH, Cl is the second most important oxidant in Delhi, with a significant contribution of 23.4 % during the morning (averaged over 07:00–09:00 LT) and 8.2 % throughout the day (06:00–16:00 LT). In Leicester, Cl is the highest contributor (74.0 %) towards AOC during the morning. In fact, with 34.1 % contribution, Cl is a major oxidant after OH during the daytime. Besides the abundance of Cl, higher reactivity enhances the contribution of Cl in AOC, which is further substantiated by the ratio of Cl reactivity to OH reactivity (Fig. 5b). This ratio indicates that Cl reactivity exceeds OH reactivity by a significant margin, ranging from 265 to 276 times greater throughout the day in Leicester. Such a substantial contribution of Cl in AOC leads to enhancements of RO_2 as seen in Fig. 3(f, l). A prominent morning (07:00–09:00 LT) peak in RO_2 is attributed to the atmospheric oxidation enhanced by Cl during that time. Notably the strongest contribution of Cl in AOC during the early morning in Leicester strengthens RO_2 peak by up to a factor of 8 (Fig. 3l). The role of Cl is predominant in Leicester as well as in Delhi during the early morning, compared to a polluted environment of Hong Kong, China, where Cl contribution was estimated to be 21.5 % (Xue et al., 2015). NO_3 and O_3 were found to play a relatively minor role in AOC at both urban environments.

4.4 Sensitivity to the $ClNO_2 + Cl^-$ reaction

In a study conducted by Haskins et al. (2019) using the reacto-diffusive length-scale framework, it was demonstrated that field and laboratory observations could be reconciled by considering an aqueous-phase reaction rate constant for the $ClNO_2 + Cl^-$ reaction on the order of $\approx 10^4\ s^{-1}$. This reaction rate constant is considerably lower (by ≈ 179 times) than reported in Roberts et al. (2008). In this context, the sensitivity simulation (NEWrate) is performed using a reaction rate coefficient of $5.6 \times 10^4\ mol^{-1}\ L\ s^{-1}$ (Haskins et al., 2019) for the $ClNO_2 + Cl^-$ reaction, for both Delhi and Leicester. As depicted in Fig. S7a, the concentration of Cl remains nearly the same in the NEWrate simulation compared to the NEW simulation over Delhi. However, there are significant changes in the concentration of $ClNO_2$, as shown in Fig. S7b. The simulated $ClNO_2$ exhibits a broader peak and is approximately 30 pmol mol^{-1} higher near sunrise in the NEWrate simulation when compared to the NEW simulation. During the nighttime, approximately 20 pmol mol^{-1} of $ClNO_2$ is simulated in the NEWrate simulation, whereas it is negligible in the NEW simulation (see Fig. 3b). Since the Cl concentration is almost similar in both the NEW and NEWrate simulations, the differences in the simulated concentrations of OH, HO_2, and RO_2 remain consistent between the NEWrate or NEW simulations and the OLD and NOCL simulations (refer to Fig. S7d, e, f and Fig. 3d, e, f). The production and loss mechanisms of Cl are similar in both the NEW and NEWrate simulations (see Fig. S8a and Fig. 4a). The contributions from $ClNO_2$ formation reactions are also similar. However, in contrast to the NEW simulation, the loss of $ClNO_2$ through photolysis becomes dominant and is ≈ 6 times greater than its loss through the $ClNO_2 + Cl^-$ reaction in the NEWrate simulation. The contribution of radicals to AOC is also similar between the NEW and NEWrate simulation, as depicted in Fig. 6a and c and Fig. S9a and c, respectively, over Delhi.

In contrast to Delhi, significant differences are seen in atmospheric composition in Leicester when the rate coefficient of the $ClNO_2 + Cl^-$ reaction is altered (as shown in Fig. S7). The peak concentration of Cl becomes ≈ 0.6 fmol mol^{-1} during the morning hours of NEWrate simulation (Fig. S7g), which is about 4 times lower than the concentration of Cl in the NEW simulation (Fig. 3g). However, due to the slower rate of $ClNO_2$ consumption with Cl^-, the simulated $ClNO_2$ using the NEWrate is significantly enhanced (by ≈ 5 times) compared to NEW simulation, reaching a maximum of about 210 pmol mol^{-1} around sunrise (see Fig. S7h). Due to lower Cl concentrations, the levels of ClONO also decrease by 3.5 times in the NEWrate simulation (as shown in Fig. S7i) compared to the NEW simulation (Fig. 3i). The dominant peak seen at sunrise in the NEW simulation for OH, HO_2, and RO_2 is significantly reduced with the lower rate of the $ClNO_2 + Cl^-$ reaction, as illustrated in Fig. S7j, k, l. Significant changes in the production and loss mechanisms of Cl and $ClNO_2$ are seen in Leicester when the reaction rate of A6 is changed, as shown in Figs. S8 and 4b. For example, in the NEWrate simulation, other reactions, including the photolysis of $ClNO_2$ and ClONO, as well as the $ClO + NO$ reaction become prominent sources of Cl (with a rate of approximately 6.0×10^5 molec $cm^{-3}\ s^{-1}$), whereas in the NEW simulation, the major source for Cl is photolysis of Cl_2. The primary source for $ClNO_2$ production remains the $Cl^- + NO_2^+$ reaction in both the NEW and NEWrate simulations. However, in the NEWrate simulation, $ClNO_2$ loss from photolysis becomes the major sink, whereas in the NEW simulation, loss from the $ClNO_2 + Cl^-$ reaction is prominent. In addition, remarkable changes in AOC are seen between the NEWrate (Fig. S9b, d) and the NEW simulation (Fig. 6b, d). In the NEWrate simulation, even though Cl remains the major oxidant, its contribution is notably reduced from 74 % (in NEW simulation) to 58.1 % during the early morning hours.

5 Summary and conclusions

Extended gas- and aqueous-phase chemistry of chlorine compounds has been added to the MECCA mechanism. It

consists of 36 gas-phase reactions (inorganic, organic, and photolysis reactions). A total of 24 aqueous-phase and heterogeneous reactions have been added, containing detailed chemistry of N_2O_5 uptake on aerosols to yield $ClNO_2$ and various other competing reactions. The updated model is applied to two different urban environments: Delhi (India) and Leicester (United Kingdom) during wintertime. The major conclusions are the following.

1. The model predicts up to 0.1 pmol mol^{-1} of NO_3 and up to 8 pmol mol^{-1} of N_2O_5 during daytime in Delhi. However, nighttime production of NO_3 and N_2O_5 is seen to be negligible primarily due of the unavailability of O_3. In contrast to Delhi, NO_3 and N_2O_5 after midnight in Leicester are $\approx$ 2.6 pmol mol^{-1} and $\approx$ 330 pmol mol^{-1}, respectively. N_2O_5 uptake on aerosols yields $ClNO_2$, which produces Cl via photolysis.

2. A sharp build-up of Cl with sunrise is mainly through Cl_2 photolysis in Delhi. Besides Cl_2, photolysis of $ClNO_2$ and ClONO and the reaction of ClO with NO are prominent Cl sources in Leicester. VOCs are the main sink for Cl at both locations, whereas NO_2 is also an important sink for Cl in Leicester. The latter results in the formation of $ClNO_2$ with a major contribution in Delhi, while $Cl^- + NO_2^+$ is a stronger source in Leicester. Photolysis is the major sink for $ClNO_2$ in Delhi; however, its uptake on chloride aerosols is a prominent sink in Leicester.

3. The magnitude of Cl ($\approx$ 750 s^{-1}) and OH ($\approx$ 25 s^{-1}) reactivities is significantly greater in Delhi, particularly during the morning hours, when compared to Leicester. However, the Cl-to-OH reactivity ratio ($\approx$ 270) is pronounced in Leicester, coinciding with higher contribution of Cl in AOC.

4. Sensitivity simulations reveal substantial post-sunrise enhancements in OH, HO_2, and RO_2 radicals, with a prominent secondary peak due to Cl chemistry. Up to 8 times higher RO_2 is simulated in Leicester primarily because of leading role of Cl in AOC potential.

It is important to note that box models, despite their general limitation of neglecting transport phenomena and assuming species to be well mixed, do include highly detailed chemical mechanisms. Furthermore, because the model is initialized with measurements of chemical species at both locations and the modeled levels align with observed data, significant discrepancies in model estimates would be unexpected. Future studies focusing on modeling vertical gradients, in particular for radical reservoir species such as HONO and $ClNO_2$ (Young et al., 2012), are recommended.

This study highlights the vital role of Cl chemistry in governing the oxidation capacity of the atmosphere and air quality, and therefore it is important to account for it in detailed photochemical as well as in 3-D chemical transport models. This will lead to better quantification of the importance of radicals in atmospheric oxidation and, hence, the formation of ozone as well as secondary aerosols over the regional to global scale. Future studies focusing on secondary aerosol formation and new particle formation from heterogeneous reactions are needed to deepen the understanding of transformation of trace gases to aerosols.

Code and data availability. CAABA/MECCA is a community box model published under the GNU General Public License, available from the GitLab repository (https://gitlab.com/RolfSander/caaba-mecca, Sander, 2023). The version of CAABA/MECCA updated in this study is currently available in the "delhi" branch of the repository. The new chlorine mechanism will be included in the next release of CAABA/MECCA. All the model outputs associated with this study are archived on Zenodo (https://zenodo.org/record/8332131, last access: 4 December 2023, Soni et al., 2023).

Supplement. The supplement related to this article is available online at: https://doi.org/10.5194/acp-23-15165-2023-supplement.

Author contributions. MS, RS, and DT designed the study with input from SSG, PL, and NO. MS, RS, and DT developed and analyzed the chemical mechanism, and MS performed the simulations. APo, RS, LKS, DT, IAG, and NO helped MS in the analyses and interpretations of the results. APa assisted MS in compiling literature and some input dataset. MS wrote the manuscript and all the co-authors contributed to the review and editing.

Competing interests. At least one of the (co-)authors is a member of the editorial board of *Atmospheric Chemistry and Physics*. The peer-review process was guided by an independent editor, and the authors also have no other competing interests to declare.

Disclaimer. Publisher's note: Copernicus Publications remains neutral with regard to jurisdictional claims made in the text, published maps, institutional affiliations, or any other geographical representation in this paper. While Copernicus Publications makes every effort to include appropriate place names, the final responsibility lies with the authors.

Acknowledgements. The authors gratefully acknowledge the use of the CAMS inventory for VOCs emissions data available from ECCAD (https://eccad.sedoo.fr/#/catalogue, last access: 4 December 2023). We thank ECMWF for the ERA5 dataset. We acknowledge UK AIR (Air Information Resource) for the chemical species data through https://uk-air.defra.gov.uk/data/ (last access: 4 December 2023). Authors thank James M. Roberts (NOAA Chemical Sciences Laboratory, USA), Tao Wang (The Hong Kong Polytechnic University, Hong Kong), Men Xia (University of Helsinki, Finland), and Renuka Soni for valuable inputs on kinetics. Meghna Soni,

Narendra Ojha, and Lokesh K. Sahu acknowledge support from the Physical Research Laboratory, Ahmedabad, a unit of the Department of Space, Government of India.

Financial support. The article processing charges for this open-access publication were covered by the Max Planck Society.

Review statement. This paper was edited by John Orlando and reviewed by three anonymous referees.

References

Atkinson, R., Baulch, D. L., Cox, R. A., Crowley, J. N., Hampson, R. F., Hynes, R. G., Jenkin, M. E., Rossi, M. J., Troe, J., and IUPAC Subcommittee: Evaluated kinetic and photochemical data for atmospheric chemistry: Volume II – gas phase reactions of organic species, Atmos. Chem. Phys., 6, 3625–4055, https://doi.org/10.5194/acp-6-3625-2006, 2006.

Atkinson, R., Baulch, D. L., Cox, R. A., Crowley, J. N., Hampson, R. F., Hynes, R. G., Jenkin, M. E., Rossi, M. J., and Troe, J.: Evaluated kinetic and photochemical data for atmospheric chemistry: Volume III – gas phase reactions of inorganic halogens, Atmos. Chem. Phys., 7, 981–1191, https://doi.org/10.5194/acp-7-981-2007, 2007.

Bannan, T. J., Booth, A. M., Bacak, A., Muller, J. B. A., Leather, K. E., Le Breton, M., Jones, B., Young, D., Coe, H., Allan, J., Visser, S., Slowik, J. G., Furger, M., Prévôt, A. S. H., Lee, J., Dunmore, R. E., Hopkins, J. R., Hamilton, J. F., Lewis, A. C., Whalley, L. K., Sharp, T., Stone, D., Heard, D. E., Fleming, Z. L., Leigh, R., Shallcross, D. E., and Percival, C. J.: The first UK measurements of nitryl chloride using a chemical ionization mass spectrometer in central London in the summer of 2012, and an investigation of the role of Cl atom oxidation, J. Geophys. Res.-Atmos., 120, 5638–5657, https://doi.org/10.1002/2014JD022629, 2015.

Behnke, W., George, C., Scheer, V., and Zetzsch, C.: Production and decay of $ClNO_2$ from the reaction of gaseous N_2O_5 with NaCl solution: Bulk and aerosol experiments, J. Geophys. Res., 102D, 3795–3804, https://doi.org/10.1029/96JD03057, 1997.

Bertram, T. H. and Thornton, J. A.: Toward a general parameterization of N2O5 reactivity on aqueous particles: the competing effects of particle liquid water, nitrate and chloride, Atmos. Chem. Phys., 9, 8351–8363, https://doi.org/10.5194/acp-9-8351-2009, 2009.

Brown, S., Stark, H., Ciciora, S., and Ravishankara, A.: In-situ Measurement of Atmospheric NO_3 and N_2O_5 via Cavity Ring-down Spectroscopy, Geophys. Res. Lett., 28, 3227–3230, https://doi.org/10.1029/2001GL013303, 2001.

Brown, S. S., Osthoff, H. D., Stark, H., Dubé, W. P., Ryerson, T. B., Warneke, C., de Gouw, J. A., Wollny, A. G., Parrish, D. D., Fehsenfeld, F. C., and Ravishankara, A.: Aircraft observations of daytime NO_3 and N_2O_5 and their implications for tropospheric chemistry, J. Photoch. Photobio. A, 176, 270–278, https://doi.org/10.1016/j.jphotochem.2005.10.004, in Honour of Professor Richard P. Wayne, 2005.

Burkholder, J. B., Sander, S. P., Abbatt, J., Barker, J. R., Huie, R. E., Kolb, C. E., Kurylo, M. J., Orkin, V. L., Wilmouth, D. M., and Wine, P. H.: Chemical Kinetics and Photochemical Data for Use in Atmospheric Studies, Evaluation No. 18, JPL Publication 15-10, Jet Propulsion Laboratory, Pasadena, http://jpldataeval.jpl.nasa.gov (last access: 4 December 2023, 2015.

Chen, Y., Beig, G., Archer-Nicholls, S., Drysdale, W., Acton, W. J. F., Lowe, D., Nelson, B., Lee, J., Ran, L., Wang, Y., Wu, Z., Sahu, S. K., Sokhi, R. S., Singh, V., Gadi, R., Nicholas Hewitt, C., Nemitz, E., Archibald, A., McFiggans, G., and Wild, O.: Avoiding high ozone pollution in Delhi, India, Faraday Discuss., 226, 502–514, https://doi.org/10.1039/D0FD00079E, 2021.

Choi, M. S., Qiu, X., Zhang, J., Wang, S., Li, X., Sun, Y., Chen, J., and Ying, Q.: Study of Secondary Organic Aerosol Formation from Chlorine Radical-Initiated Oxidation of Volatile Organic Compounds in a Polluted Atmosphere Using a 3D Chemical Transport Model, Environ. Sci. Technol., 54, 13409–13418, https://doi.org/10.1021/acs.est.0c02958, 2020.

Coombes, R. G., Golding, J. G., and Hadjigeorgiou, P.: Electrophilic aromatic substitution. Part 23. The nitration of phenol and the cresols in aqueous sulphuric acid, J. Chem. Soc. Perkin Trans. 2, 1451–1459, https://doi.org/10.1039/P29790001451, 1979.

Elshorbany, Y. F., Kurtenbach, R., Wiesen, P., Lissi, E., Rubio, M., Villena, G., Gramsch, E., Rickard, A. R., Pilling, M. J., and Kleffmann, J.: Oxidation capacity of the city air of Santiago, Chile, Atmos. Chem. Phys., 9, 2257–2273, https://doi.org/10.5194/acp-9-2257-2009, 2009.

Fan, J. and Zhang, R.: Atmospheric Oxidation Mechanism of Isoprene, Environ. Chem., 1, 140–149, https://doi.org/10.1071/EN04045, 2004.

Faxon, C. and Allen, D.: Chlorine chemistry in urban atmospheres: A review, Environ. Chem., 10, 221–233, https://doi.org/10.1071/EN13026, 2013.

Fickert, S., Helleis, F., Adams, J. W., Moortgat, G. K., and Crowley, J. N.: Reactive uptake of $ClNO_2$ on aqueous bromide solutions, J. Phys. Chem. A, 102, 10689–10696, https://doi.org/10.1021/JP983004N, 1998.

Frenzel, A., Scheer, V., Sikorski, R., C., G., Behnke, W., and Zetzsch, C.: Heterogeneous interconversion reactions of $BrNO_2$, $ClNO_2$, Br_2, and Cl_2, J. Phys. Chem. A, 102, 1329–1337, https://doi.org/10.1021/JP973044B, 1998.

Fried, A., Henry, B. E., Calvert, J. G., and Michael, M.: The reaction probability of N_2O_5 with sulfuric acid aerosols at stratospheric temperatures and compositions, J. Geophys. Res., 99D, 3517–3532, https://doi.org/10.1029/93JD01907, 1994.

Geyer, A., Alicke, B., Ackermann, R., Martinez, M., Harder, H., Brune, W., di Carlo, P., Williams, E., Jobson, T., Hall, S., Shetter, R., and Stutz, J.: Direct observations of daytime NO_3: Implications for urban boundary layer chemistry, J. Geophys. Res.-Atmos., 108, 4368, https://doi.org/10.1029/2002JD002967, 2003.

Ghosh, B., Papanastasiou, D. K., Talukdar, R. K., Roberts, J. M., and Burkholder, J. B.: Nitryl Chloride (ClNO2): UV/Vis Absorption Spectrum between 210 and 296 K and O(3P) Quantum Yield at 193 and 248 nm, The J. Phys. Chem. A, 116, 5796–5805, https://doi.org/10.1021/jp207389y, 2012.

Golden, D. M.: The Reaction Cl + NO_2 → ClONO and $ClNO_2$, The J. Phys. Chem. A, 111, 6772–6780, https://doi.org/10.1021/jp069000x, 2007.

Granier, C., Darras, S., van der Gon, H. D., Doubalova, J., Elguindi, N., Galle, B., Gauss, M., Guevara, M., Jalkanen, J.-P., Kuenen, J., Liousse, C., Quack, B., Simpson, D., and Sindelarova, K.: The Copernicus Atmosphere Monitoring Service global and regional emissions (April 2019 version), Copernicus Atmosphere Monitoring Service (CAMS) report, https://doi.org/10.24380/d0bn-kx16, 2019.

Green, M., Yarwood, G., and Niki, H.: FTIR study of the Cl-atom initiated oxidation of methylglyoxal, Int. J. Chem. Kinet., 22, 689–699, https://doi.org/10.1002/KIN.550220705, 1990.

Grigorev, A. E., Makarov, I. E., and Pikaev, A. K.: Formation of Cl_2^- in the bulk solution during the radiolysis of concentrated aqueous solutions of chlorides, High Energy Chem., 21, 99–102, https://kinetics.nist.gov/solution/Detail?id=1987GRI/MAK99-102:2 (last access: 4 December 2023), 1987.

Gunthe, S., Liu, P., Panda, U., S Raj, S., Sharma, A., Darbyshire, E., Reyes Villegas, E., Allan, J., Chen, Y., Wang, X., Song, S., Pohlker, M., Shi, L., Wang, Y., Kommula, S., Liu, T., Ravikrishna, R., Mcfiggans, G., Mickley, L., and Coe, H.: Enhanced aerosol particle growth sustained by high continental chlorine emission in India, Nat. Geosci., 14, 77–84, https://doi.org/10.1038/s41561-020-00677-x, 2021.

Haskins, J. D., Lee, B. H., Lopez-Hilifiker, F. D., Peng, Q., Jaeglé, L., Reeves, J. M., Schroder, J. C., Campuzano-Jost, P., Fibiger, D., McDuffie, E. E., Jiménez, J. L., Brown, S. S., and Thornton, J. A.: Observational Constraints on the Formation of Cl2 From the Reactive Uptake of $ClNO_2$ on Aerosols in the Polluted Marine Boundary Layer, J. Geophys. Res.-Atmos., 124, 8851–8869, https://doi.org/10.1029/2019JD030627, 2019.

Haslett, S. L., Bell, D. M., Kumar, V., Slowik, J. G., Wang, D. S., Mishra, S., Rastogi, N., Singh, A., Ganguly, D., Thornton, J., Zheng, F., Li, Y., Nie, W., Liu, Y., Ma, W., Yan, C., Kulmala, M., Daellenbach, K. R., Hadden, D., Baltensperger, U., Prevot, A. S. H., Tripathi, S. N., and Mohr, C.: Nighttime NO emissions strongly suppress chlorine and nitrate radical formation during the winter in Delhi, Atmos. Chem. Phys., 23, 9023–9036, https://doi.org/10.5194/acp-23-9023-2023, 2023.

Heal, M. R., Harrison, M. A. J., and Cape, J. N.: Aqueous-phase nitration of phenol by N_2O_5 and $ClNO_2$, Atmos. Environ., 41, 3515–3520, https://doi.org/10.1016/J.ATMOSENV.2007.02.003, 2007.

Hens, K., Novelli, A., Martinez, M., Auld, J., Axinte, R., Bohn, B., Fischer, H., Keronen, P., Kubistin, D., Nölscher, A. C., Oswald, R., Paasonen, P., Petäjä, T., Regelin, E., Sander, R., Sinha, V., Sipilä, M., Taraborrelli, D., Tatum Ernest, C., Williams, J., Lelieveld, J., and Harder, H.: Observation and modelling of HO_x radicals in a boreal forest, Atmos. Chem. Phys., 14, 8723–8747, https://doi.org/10.5194/acp-14-8723-2014, 2014.

Hersbach, H., Bell, B., Berrisford, P., Hirahara, S., Horányi, A., Muñoz-Sabater, J., Nicolas, J., Peubey, C., Radu, R., Schepers, D., Simmons, A., Soci, C., Abdalla, S., Abellan, X., Balsamo, G., Bechtold, P., Biavati, G., Bidlot, J., Bonavita, M., De Chiara, G., Dahlgren, P., Dee, D., Diamantakis, M., Dragani, R., Flemming, J., Forbes, R., Fuentes, M., Geer, A., Haimberger, L., Healy, S., Hogan, R. J., Hólm, E., Janisková, M., Keeley, S., Laloyaux, P., Lopez, P., Lupu, C., Radnoti, G., de Rosnay, P., Rozum, I., Vamborg, F., Villaume, S., and Thépaut, J.-N.: The ERA5 global reanalysis, Q. J. Roy. Meteorol. Soc., 146, 1999–2049, https://doi.org/10.1002/qj.3803, 2020.

Horowitz, L. W., Fiore, A. M., Milly, G. P., Cohen, R. C., Perring, A., Wooldridge, P. J., Hess, P. G., Emmons, L. K., and Lamarque, J.-F.: Observational constraints on the chemistry of isoprene nitrates over the eastern United States, J. Geophys. Res.-Atmos., 112, D12S08, https://doi.org/10.1029/2006JD007747, 2007.

Hossaini, R., Chipperfield, M. P., Saiz-Lopez, A., Fernandez, R., Monks, S., Feng, W., Brauer, P., and von Glasow, R.: A global model of tropospheric chlorine chemistry: Organic versus inorganic sources and impact on methane oxidation, J. Geophys. Res.-Atmos., 121, 14271–14297, https://doi.org/10.1002/2016JD025756, 2016.

Iraci, L. T., Riffel, B. G., Robinson, C. B., Michelsen, R. R., and Stephenson, R. M.: The acid catalyzed nitration of methanol: formation of methyl nitrate via aerosol chemistry, J. Atmos. Chem., 58, 253–266, https://doi.org/10.1007/S10874-007-9091-9, 2007.

Janowski, B., Knauth, H.-D., and Martin, H.: Chlornitrit, ein metastabiles Zwischenprodukt der Reaktion von Dichlormonoxid mit Nitrosylchlorid, Berichte der Bunsengesellschaft für physikalische Chemie, 81, 1262–1270, https://doi.org/10.1002/bbpc.19770811212, 1977.

Khan, A., Morris, W., Watson, L., Galloway, M., Hamer, P., Shallcross, B., Percival, C., and Shallcross, D.: Estimation of Daytime NO3 Radical Levels in the UK Urban Atmosphere Using the Steady State Approximation Method, Adv. Meteorol., 2015, 9, https://doi.org/10.1155/2015/294069, 2015a.

Khan, M., Cooke, M., Utembe, S., Archibald, A., Derwent, R., Xiao, P., Percival, C., Jenkin, M., Morris, W., and Shallcross, D.: Global modeling of the nitrate radical (NO3) for present and pre-industrial scenarios, Atmos. Res., 164-165, 347–357, https://doi.org/10.1016/j.atmosres.2015.06.006, 2015b.

Knipping, E. M., Lakin, M. J., Foster, K. L., Jungwirth, P., Tobias, D. J., Gerber, R. B., Dabdub, D., and Finlayson-Pitts, B. J.: Experiments and simulations of ion-enhanced interfacial chemistry on aqueous NaCl aerosols, Science, 288, 301–306, https://doi.org/10.1126/SCIENCE.288.5464.301, 2000.

Kroflič, A., Grilc, M., and Grgić, I.: Unraveling Pathways of Guaiacol Nitration in Atmospheric Waters: Nitrite, A Source of Reactive Nitronium Ion in the Atmosphere, Environ. Sci. Technol., 49, 9150–9158, https://doi.org/10.1021/acs.est.5b01811, 2015.

Landgraf, J. and Crutzen, P. J.: An efficient method for online calculations of photolysis and heating rates, J. Atmos. Sci., 55, 863–878, https://doi.org/10.1175/1520-0469(1998)055<0863:AEMFOC>2.0.CO;2, 1998.

Lanz, V. A., Prévôt, A. S. H., Alfarra, M. R., Weimer, S., Mohr, C., DeCarlo, P. F., Gianini, M. F. D., Hueglin, C., Schneider, J., Favez, O., D'Anna, B., George, C., and Baltensperger, U.: Characterization of aerosol chemical composition with aerosol mass spectrometry in Central Europe: an overview, Atmos. Chem. Phys., 10, 10453–10471, https://doi.org/10.5194/acp-10-10453-2010, 2010.

Lawler, M. J., Sander, R., Carpenter, L. J., Lee, J. D., von Glasow, R., Sommariva, R., and Saltzman, E. S.: HOCl and Cl2 observations in marine air, Atmos. Chem. Phys., 11, 7617–7628, https://doi.org/10.5194/acp-11-7617-2011, 2011.

Liao, J., Huey, L., Liu, Z., Tanner, D., Cantrell, C., Orlando, J., Flocke, F., Shepson, P., Weinheimer, A., Hall, S., Ullmann, K., Beine, H., Wang, Y., Ingall, E., Stephens, C., Hornbrook, R., Apel, E., Riemer, D., Fried, A., and Nowak, J.: High levels of

molecular chlorine in the Arctic atmosphere, Nat. Geosci., 7, 91–94, https://doi.org/10.1038/ngeo2046, 2014.

Liu, X., Qu, H., Huey, L. G., Wang, Y., Sjostedt, S., Zeng, L., Lu, K., Wu, Y., Hu, M., Shao, M., Zhu, T., and Zhang, Y.: High Levels of Daytime Molecular Chlorine and Nitryl Chloride at a Rural Site on the North China Plain, Environ. Sci. Technol., 51, 9588–9595, https://doi.org/10.1021/acs.est.7b03039, 2017.

Lobert, J. M., Keene, W. C., Logan, J. A., and Yevich, R.: Global chlorine emissions from biomass burning: Reactive Chlorine Emissions Inventory, J. Geophys. Res.-Atmos., 104, 8373–8389, https://doi.org/10.1029/1998JD100077, 1999.

Müller, B. and Heal, M. R.: The Henry's law coefficient of 2-nitrophenol over the temperature range 278–303 K, Chemosphere, 45, 309–314, https://doi.org/10.1016/S0045-6535(00)00592-0, 2001.

Nakoudi, K., Giannakaki, E., Dandou, A., Tombrou, M., and Komppula, M.: Planetary boundary layer height by means of lidar and numerical simulations over New Delhi, India, Atmos. Meas. Tech., 12, 2595–2610, https://doi.org/10.5194/amt-12-2595-2019, 2019.

Nelson, B. S., Stewart, G. J., Drysdale, W. S., Newland, M. J., Vaughan, A. R., Dunmore, R. E., Edwards, P. M., Lewis, A. C., Hamilton, J. F., Acton, W. J., Hewitt, C. N., Crilley, L. R., Alam, M. S., Şahin, Ü. A., Beddows, D. C. S., Bloss, W. J., Slater, E., Whalley, L. K., Heard, D. E., Cash, J. M., Langford, B., Nemitz, E., Sommariva, R., Cox, S., Shivani, Gadi, R., Gurjar, B. R., Hopkins, J. R., Rickard, A. R., and Lee, J. D.: In situ ozone production is highly sensitive to volatile organic compounds in Delhi, India, Atmos. Chem. Phys., 21, 13609–13630, https://doi.org/10.5194/acp-21-13609-2021, 2021.

Nelson, B. S., Bryant, D. J., Alam, M. S., Sommariva, R., Bloss, W. J., Newland, M. J., Drysdale, W. S., Vaughan, A. R., Acton, W. J. F., Hewitt, C. N., Crilley, L. R., Swift, S. J., Edwards, P. M., Lewis, A. C., Langford, B., Nemitz, E., Shivani, Gadi, R., Gurjar, B. R., Heard, D. E., Whalley, L. K., Sahin, U. A., Beddows, D. C. S., Hopkins, J. R., Lee, J. D., Rickard, A. R., and Hamilton, J. F.: Extreme Concentrations of Nitric Oxide Control Daytime Oxidation and Quench Nocturnal Oxidation Chemistry in Delhi during Highly Polluted Episodes, Environ. Sci. Technol. Lett., 10, 520–527, https://doi.org/10.1021/acs.estlett.3c00171, 2023.

Niki, H., Maker, P., Savage, C., and Breitenbach, L.: Fourier transform IR spectroscopic observation of chlorine nitrite, ciono, formed via Cl + NO_2 (+M) → ClONO(+M), Chem. Phys. Lett., 59, 78–79, https://doi.org/10.1016/0009-2614(78)85618-8, 1978.

Niki, H., Maker, P. D., Savage, C. M., and Breitenbach, L. P.: An FTIR study of the Cl-atom-initiated reaction of glyoxal, Int. J. Chem. Kinet., 17, 547–558, https://doi.org/10.1002/KIN.550170507, 1985.

Niki, H., Maker, P. D., Savage, C. M., and Hurley, M. D.: Fourier transform infrared study of the kinetics and mechanisms for the Cl-atom- and HO-radical-initiated oxidation of glycolaldehyde, J. Phys. Chem., 91, 2174–2178, https://doi.org/10.1021/J100292A038, 1987.

Nölscher, A., Butler, T., Auld, J., Veres, P., Muñoz, A., Taraborrelli, D., Vereecken, L., Lelieveld, J., and Williams, J.: Using total OH reactivity to assess isoprene photooxidation via measurement and model, Atmos. Environ., 89, 453–463, https://doi.org/10.1016/j.atmosenv.2014.02.024, 2014.

Osthoff, H. D., Roberts, J. M., Ravishankara, A. R., Williams, E. J., Lerner, B. M., Sommariva, R., Bates, T. S., Coffman, D., Quinn, P. K., Dibb, J. E., Stark, H., Burkholder, J. B., Talukdar, R. K., Meagher, J., Fehsenfeld, F. C., and Brown, S. S.: High levels of nitryl chloride in the polluted subtropical marine boundary layer, Nat. Geosci., 1, 324–328, https://doi.org/10.1038/NGEO177, 2008.

Pawar, P. V., Ghude, S. D., Govardhan, G., Acharja, P., Kulkarni, R., Kumar, R., Sinha, B., Sinha, V., Jena, C., Gunwani, P., Adhya, T. K., Nemitz, E., and Sutton, M. A.: Chloride (HCl/Cl^-) dominates inorganic aerosol formation from ammonia in the Indo-Gangetic Plain during winter: modeling and comparison with observations, Atmos. Chem. Phys., 23, 41–59, https://doi.org/10.5194/acp-23-41-2023, 2023.

Pozzer, A., Reifenberg, S. F., Kumar, V., Franco, B., Kohl, M., Taraborrelli, D., Gromov, S., Ehrhart, S., Jöckel, P., Sander, R., Fall, V., Rosanka, S., Karydis, V., Akritidis, D., Emmerichs, T., Crippa, M., Guizzardi, D., Kaiser, J. W., Clarisse, L., Kiendler-Scharr, A., Tost, H., and Tsimpidi, A.: Simulation of organics in the atmosphere: evaluation of EMACv2.54 with the Mainz Organic Mechanism (MOM) coupled to the ORACLE (v1.0) submodel, Geosci. Model Dev., 15, 2673–2710, https://doi.org/10.5194/gmd-15-2673-2022, 2022.

Qiu, X., Ying, Q., Wang, S., Duan, L., Wang, Y., Lu, K., Wang, P., Xing, J., Zheng, M., Zhao, M., Zheng, H., Zhang, Y., and Hao, J.: Significant impact of heterogeneous reactions of reactive chlorine species on summertime atmospheric ozone and free-radical formation in north China, Sci. Total Environ., 693, 133580, https://doi.org/10.1016/J.SCITOTENV.2019.133580, 2019a.

Qiu, X., Ying, Q., Wang, S., Duan, L., Zhao, J., Xing, J., Ding, D., Sun, Y., Liu, B., Shi, A., Yan, X., Xu, Q., and Hao, J.: Modeling the impact of heterogeneous reactions of chlorine on summertime nitrate formation in Beijing, China, Atmos. Chem. Phys., 19, 6737–6747, https://doi.org/10.5194/acp-19-6737-2019, 2019b.

Ragains, M. L. and Finlayson-Pitts, B. J.: Kinetics and Mechanism of the Reaction of Cl Atoms with 2-Methyl-1,3-butadiene (Isoprene) at 298 K, The J. Phys. Chem. A, 101, 1509–1517, https://doi.org/10.1021/jp962786m, 1997.

Ravishankara, A. R.: Are chlorine atoms significant tropospheric free radicals?, P. Natl. Acad. Sci. USA, 106, 13639–13640, https://doi.org/10.1073/pnas.0907089106, 2009.

Rickard, A.: Master Chemical Mechanism, MCM v3.3.1, http://mcm.york.ac.uk (last access: 4 December 2023), 2009.

Riedel, T. P., Wolfe, G. M., Danas, K. T., Gilman, J. B., Kuster, W. C., Bon, D. M., Vlasenko, A., Li, S.-M., Williams, E. J., Lerner, B. M., Veres, P. R., Roberts, J. M., Holloway, J. S., Lefer, B., Brown, S. S., and Thornton, J. A.: An MCM modeling study of nitryl chloride ($ClNO_2$) impacts on oxidation, ozone production and nitrogen oxide partitioning in polluted continental outflow, Atmos. Chem. Phys., 14, 3789–3800, https://doi.org/10.5194/acp-14-3789-2014, 2014.

Roberts, J. M., Osthoff, H. D., Brown, S. S., and Ravishankara, A. R.: N_2O_5 oxidizes chloride to Cl_2 in acidic atmospheric aerosol, Science, 321, 1059, https://doi.org/10.1126/SCIENCE.1158777, 2008.

Roberts, J. M., Osthoff, H. D., Brown, S. S., Ravishankara, A. R., Coffman, D., Quinn, P., and Bates, T.: Laboratory studies of products of N_2O_5 uptake on Cl-containing substrates, Geophys.

Res. Lett., 36, L20808, https://doi.org/10.1029/2009GL040448, 2009.

Rosanka, S., Sander, R., Wahner, A., and Taraborrelli, D.: Oxidation of low-molecular-weight organic compounds in cloud droplets: development of the Jülich Aqueous-phase Mechanism of Organic Chemistry (JAMOC) in CAABA/MECCA (version 4.5.0), Geosci. Model Dev., 14, 4103–4115, https://doi.org/10.5194/gmd-14-4103-2021, 2021.

Ryder, O. S., Campbell, N. R., Shaloski, M., Al-Mashat, H., Nathanson, G. M., and Bertram, T. H.: Role of organics in regulating $ClNO_2$ production at the air-sea interface, J. Phys. Chem. A, 119, 8519–8526, https://doi.org/10.1021/JP5129673, 2015.

Saiz-Lopez, A. and von Glasow, R.: Reactive halogen chemistry in the troposphere, Chem. Soc. Rev., 41, 6448–6472, https://doi.org/10.1039/C2CS35208G, 2012.

Sander, R.: Compilation of Henry's law constants (version 4.0) for water as solvent, Atmos. Chem. Phys., 15, 4399–4981, https://doi.org/10.5194/acp-15-4399-2015, 2015.

Sander, R.: CAABA/MECCA [code], GitLab repository, https://gitlab.com/RolfSander/ (last access: 4 December 2023), 2023.

Sander, R., Jöckel, P., Kirner, O., Kunert, A. T., Landgraf, J., and Pozzer, A.: The photolysis module JVAL-14, compatible with the MESSy standard, and the JVal PreProcessor (JVPP), Geosci. Model Dev., 7, 2653–2662, https://doi.org/10.5194/gmd-7-2653-2014, 2014.

Sander, R., Baumgaertner, A., Cabrera-Perez, D., Frank, F., Gromov, S., Grooß, J.-U., Harder, H., Huijnen, V., Jöckel, P., Karydis, V. A., Niemeyer, K. E., Pozzer, A., Riede, H., Schultz, M. G., Taraborrelli, D., and Tauer, S.: The community atmospheric chemistry box model CAABA/MECCA-4.0, Geosci. Model Dev., 12, 1365–1385, https://doi.org/10.5194/gmd-12-1365-2019, 2019.

Sandu, A. and Sander, R.: Technical note: Simulating chemical systems in Fortran90 and Matlab with the Kinetic PreProcessor KPP-2.1, Atmos. Chem. Phys., 6, 187–195, https://doi.org/10.5194/acp-6-187-2006, 2006.

Sapoli, M., De Santis, A., Marziano, N. C., Pinna, F., and Zingales, A.: Equilibria of nitric acid in sulfuric and perchloric acid at 25.degree.C by Raman and UV spectroscopy, The J. Phys. Chem., 89, 2864–2869, https://doi.org/10.1021/j100259a032, 1985.

Sarwar, G., Simon, H., Xing, J., and Mathur, R.: Importance of tropospheric $ClNO_2$ chemistry across the Northern Hemisphere, Geophys. Res. Lett., 41, 4050–4058, https://doi.org/10.1002/2014GL059962, 2014.

Seinfeld, J. H. and Pandis, S. N.: Atmospheric Chemistry and Physics, John Wiley & Sons, Inc., ISBN 9781119221173, 2016.

Sharma, G., Sinha, B., Pallavi, Hakkim, H., Chandra, B. P., Kumar, A., and Sinha, V.: Gridded Emissions of CO, NO_x, SO_2, CO_2, NH_3, HCl, CH_4, $PM_{2.5}$, PM_{10}, BC, and NMVOC from Open Municipal Waste Burning in India, Environ. Sci. Technol., 53, 4765–4774, https://doi.org/10.1021/acs.est.8b07076, 2019.

Shi, J. and Bernhard, M. J.: Kinetic studies of Cl-atom reactions with selected aromatic compounds using the photochemical reactor-FTIR spectroscopy technique, Int. J. Chem. Kinet., 29, 349–358, https://doi.org/10.1002/(SICI)1097-4601(1997)29:5<349::AID-KIN5>3.0.CO;2-U, 1997.

Sindelarova, K., Granier, C., Bouarar, I., Guenther, A., Tilmes, S., Stavrakou, T., Müller, J.-F., Kuhn, U., Stefani, P., and Knorr, W.: Global data set of biogenic VOC emissions calculated by the MEGAN model over the last 30 years, Atmos. Chem. Phys., 14, 9317–9341, https://doi.org/10.5194/acp-14-9317-2014, 2014.

Sokolov, O., Hurley, M. D., Ball, J. C., Wallington, T. J., Nelsen, W., Barnes, I., and Becker, K. H.: Kinetics of the reactions of chlorine atoms with CH_3ONO and CH_3ONO_2, Int. J. Chem. Kinet., 31, 357–359, https://doi.org/10.1002/(SICI)1097-4601(1999)31:5<357::AID-KIN5>3.0.CO;2-6, 1999.

Sommariva, R., Hollis, L. D. J., Sherwen, T., Baker, A. R., Ball, S. M., Bandy, B. J., Bell, T. G., Chowdhury, M. N., Cordell, R. L., Evans, M. J., Lee, J. D., Reed, C., Reeves, C. E., Roberts, J. M., Yang, M., and Monks, P. S.: Seasonal and geographical variability of nitryl chloride and its precursors in Northern Europe, Atmos. Sci. Lett., 19, e844, https://doi.org/10.1002/asl.844, 2018.

Sommariva, R., Crilley, L. R., Ball, S. M., Cordell, R. L., Hollis, L. D., Bloss, W. J., and Monks, P. S.: Enhanced wintertime oxidation of VOCs via sustained radical sources in the urban atmosphere, Environ. Pollut., 274, 116563, https://doi.org/10.1016/j.envpol.2021.116563, 2021.

Soni, M., Sander, R., Taraborrelli, D., and Ojha, N.: Model outputs associated with "Comprehensive multiphase chlorine chemistry in the box model CAABA/MECCA: Implications to atmospheric oxidative capacity" [data set], Zenodo, https://doi.org/10.5281/zenodo.8332131, 2023.

Staudt, S., Gord, J. R., Karimova, N. V., McDuffie, E. E., Brown, S. S., Gerber, R. B., Nathanson, G. M., and Bertram, T. H.: Sulfate and carboxylate suppress the formation of $ClNO_2$ at atmospheric interfaces, Earth Space Chem., 3, 1987–1997, https://doi.org/10.1021/ACSEARTHSPACECHEM.9B00177, 2019.

Taraborrelli, D., Lawrence, M. G., Crowley, J. N., Dillon, T. J., Gromov, S., Groß, C. B. M., Vereecken, L., and Lelieveld, J.: Hydroxyl radical buffered by isoprene oxidation over tropical forests, Nat. Geosci., 5, 190–193, https://doi.org/10.1038/NGEO1405, 2012.

Taraborrelli, D., Cabrera-Perez, D., Bacer, S., Gromov, S., Lelieveld, J., Sander, R., and Pozzer, A.: Influence of aromatics on tropospheric gas-phase composition, Atmos. Chem. Phys., 21, 2615–2636, https://doi.org/10.5194/acp-21-2615-2021, 2021.

Tham, Y. J., Wang, Z., Li, Q., Yun, H., Wang, W., Wang, X., Xue, L., Lu, K., Ma, N., Bohn, B., Li, X., Kecorius, S., Größ, J., Shao, M., Wiedensohler, A., Zhang, Y., and Wang, T.: Significant concentrations of nitryl chloride sustained in the morning: investigations of the causes and impacts on ozone production in a polluted region of northern China, Atmos. Chem. Phys., 16, 14959–14977, https://doi.org/10.5194/acp-16-14959-2016, 2016.

Thiault, G., Mellouki, A., and Bras, G. L.: Kinetics of gas phase reactions of OH and Cl with aromatic aldehydes, Phys. Chem. Chem. Phys., 4, 2194–2199, https://doi.org/10.1039/b200609j, 2002.

Thornton, J., Kercher, J., Riedel, T., Wagner, N., Cozic, J., Holloway, J., Dubé, W., Wolfe, G., Quinn, P., Middlebrook, A., Alexander, B., and Brown, S.: A large atomic chlorine source inferred from mid-continental reactive nitrogen chemistry, Nature, 464, 271–274, https://doi.org/10.1038/nature08905, 2010.

Tripathi, N., Sahu, L. K., Wang, L., Vats, P., Soni, M., Kumar, P., Satish, R. V., Bhattu, D., Sahu, R., Patel, K., Rai, P., Kumar, V., Rastogi, N., Ojha, N., Tiwari, S., Ganguly, D., Slowik, J., Prévôt, A. S. H., and Tripathi, S. N.: Characteristics of VOC

Composition at Urban and Suburban Sites of New Delhi, India in Winter, J. Geophys. Res.-Atmos., 127, e2021JD035342, https://doi.org/10.1029/2021JD035342, 2022.

von Glasow, R. and Crutzen, P.: Tropospheric Halogen Chemistry, in: Treatise on Geochemistry, edited by: Holland, H. D. and Turekian, K. K., Pergamon, Oxford, ISBN 9780080450919, 2007.

Wang, L., Arey, J., and Atkinson, R.: Reactions of chlorine atoms with a series of aromatic hydrocarbons, Environ. Sci. Technol., 39, 5302–5310, https://doi.org/10.1021/ES0479437, 2005.

Wang, T., Tham, Y. J., Xue, L., Li, Q., Zha, Q., Wang, Z., Poon, S. C. N., Dubé, W. P., Blake, D. R., Louie, P. K. K., Luk, C. W. Y., Tsui, W., and Brown, S. S.: Observations of nitryl chloride and modeling its source and effect on ozone in the planetary boundary layer of southern China, J. Geophys. Res.-Atmos., 121, 2476–2489, https://doi.org/10.1002/2015JD024556, 2016.

Wennberg, P. O., Bates, K. H., Crounse, J. D., Dodson, L. G., McVay, R. C., Mertens, L. A., Nguyen, T. B., Praske, E., Schwantes, R. H., Smarte, M. D., St Clair, J. M., Teng, A. P., Zhang, X., and Seinfeld, J. H.: Gas-Phase Reactions of Isoprene and Its Major Oxidation Products, Chem. Rev., 118, 3337–3390, https://doi.org/10.1021/acs.chemrev.7b00439, 2018.

Xue, L. K., Saunders, S. M., Wang, T., Gao, R., Wang, X. F., Zhang, Q. Z., and Wang, W. X.: Development of a chlorine chemistry module for the Master Chemical Mechanism, Geosci. Model Dev., 8, 3151–3162, https://doi.org/10.5194/gmd-8-3151-2015, 2015.

Young, C. J., Washenfelder, R. A., Roberts, J. M., Mielke, L. H., Osthoff, H. D., Tsai, C., Pikelnaya, O., Stutz, J., Veres, P. R., Cochran, A. K., VandenBoer, T. C., Flynn, J., Grossberg, N., Haman, C. L., Lefer, B., Stark, H., Graus, M., de Gouw, J., Gilman, J. B., Kuster, W. C., and Brown, S. S.: Vertically Resolved Measurements of Nighttime Radical Reservoirs in Los Angeles and Their Contribution to the Urban Radical Budget, Environ. Sci. Technol., 46, 10965–10973, https://doi.org/10.1021/es302206a, pMID: 23013316, 2012.

Zhang, B., Shen, H., Yun, X., Zhong, Q., Henderson, B. H., Wang, X., Shi, L., Gunthe, S. S., Huey, L. G., Tao, S., Russell, A. G., and Liu, P.: Global Emissions of Hydrogen Chloride and Particulate Chloride from Continental Sources, Environ. Sci. Technol., 56, 3894–3904, https://doi.org/10.1021/acs.est.1c05634, 2022.

Zhang, L., Li, Q., Wang, T., Ahmadov, R., Zhang, Q., Li, M., and Lv, M.: Combined impacts of nitrous acid and nitryl chloride on lower-tropospheric ozone: new module development in WRF-Chem and application to China, Atmos. Chem. Phys., 17, 9733–9750, https://doi.org/10.5194/acp-17-9733-2017, 2017.

Zhang, Q., Jimenez, J. L., Canagaratna, M. R., Allan, J. D., Coe, H., Ulbrich, I., Alfarra, M. R., Takami, A., Middlebrook, A. M., Sun, Y. L., Dzepina, K., Dunlea, E., Docherty, K., DeCarlo, P. F., Salcedo, D., Onasch, T., Jayne, J. T., Miyoshi, T., Shimono, A., Hatakeyama, S., Takegawa, N., Kondo, Y., Schneider, J., Drewnick, F., Borrmann, S., Weimer, S., Demerjian, K., Williams, P., Bower, K., Bahreini, R., Cottrell, L., Griffin, R. J., Rautiainen, J., Sun, J. Y., Zhang, Y. M., and Worsnop, D. R.: Ubiquity and dominance of oxygenated species in organic aerosols in anthropogenically-influenced Northern Hemisphere midlatitudes, Geophys. Res. Lett., 34, L13801, https://doi.org/10.1029/2007GL029979, 2007.